NATIONAL ADVISORY COMMITTEE FOR AERONAUTICS

TECHNICAL NOTE 2812

EFFECTS OF CYCLIC LOADING ON MECHANICAL BEHAVIOR OF 24S-T4 AND 75S-T6 ALUMINUM ALLOYS AND SAE 4130 STEEL

By C. W. MacGregor and N. Grossman

Massachusetts Institute of Technology

Washington

October 1952

1F

NATIONAL ADVISORY COMMITTEE FOR AERONAUTICS

TECHNICAL NOTE 2812

EFFECTS OF CYCLIC LOADING ON MECHANICAL BEHAVIOR OF 24S-T4 AND 75S-T6 ALUMINUM ALLOYS AND SAE 4130 STEEL

By C. W. MacGregor and N. Grossman

SUMMARY

An investigation was conducted to determine the effects of cyclic loading on the mechanical behavior of 24S-T4 and 75S-T6 aluminum alloys and SAE 4130 steel. Specimens of the three materials were subjected to various numbers of prior fatigue cycles both below and above the fatigue limits. Special slow-bend tests at constant deflection rates and temperatures were employed to show the effects of prior cycles of fatigue stressing on the transition temperature to brittle fracture for SAE 4130 steel and on the energy-absorption capacity of the aluminum alloys. Micrographic studies were made to observe and measure crack formation and propagation and additional special tests were conducted to supplement the results of the slow-bend tests. These included Charpy impact tests, microhardness surveys, tension tests, and fretting-corrosion studies.

INTRODUCTION

Previous tests (reference 1) conducted by the authors have shown that prior cycles of fatigue markedly raised the brittle transition temperature of SAE 1020 steel. This has the practical effect of seriously reducing the energy-absorption capacity of the metal, placing it in a vulnerable condition where shocks or transient overloads may produce a brittle fracture in a normally ductile steel. The special testing technique to be described showed its extreme sensitivity in detecting early damage.

It is the purpose of the present investigation to utilize this method in detecting any change in properties of 24S-T4 and 75S-T6 aluminum alloys and SAE 4130 steel due to prior fatigue. In testing the aluminum alloys it was realized that these metals might well not show an actual transition temperature, at least within the range of strain rates and temperatures available with the present equipment. Nevertheless, the primary purpose of studying these metals by this method was

to determine whether the special slow-bend test would distinguish in any way between these two alloys. With the SAE 4130 steel it was expected that actual transition temperatures would be determined.

This report will describe the special slow-bend technique utilized to show the effects of prior fatigue cycles on certain material properties, the results obtained, and supplementary tests such as Charpy impact, tension, microhardness, and fretting-corrosion tests. The effects of heat treatment on the test results will also be described.

This investigation was conducted at the Massachusetts Institute of Technology under the sponsorship and with the financial assistance of the National Advisory Committee for Aeronautics. The work to determine the effect of heat treatment on the energy-absorption capacities of the two aluminum alloys was done in the Metallurgy Department of M.I.T. by Mr. Robert E. Donovan, under the supervision of Professor Carl F. Floe, in partial fulfillment of the requirements for the B.S. degree. The section of the report entitled "Fretting Corrosion" was prepared by Mr. W. D. Tierney of the Mechanical Engineering Department. The authors wish to express their appreciation to Professor Floe for the photomicrographic crack studies and to Mr. F. M. Howell, Aluminum Company of America, who was instrumental in obtaining the aluminum alloys with complete mill history and test data.

MATERIALS AND SPECIMENS

Two commercial aluminum alloys (24S-T4 and 75S-T6) and an aircraft quality alloy steel (SAE 4130) were used in the present investigation. The rods were obtained in 1/2-inch-diameter stock from the Aluminum Company of America and the Carnegie-Illinois Steel Corp., respectively. Table I lists the chemical analyses and mechanical properties; figures 1 and 2 show the photomicrographs.

Fatigue specimens were then machined from the three materials to the dimensions given in figure 3. The surfaces of the specimens exclusive of the notches were finished with No. 0 emery cloth. The notches, situated in the centers of the test pieces, were turned with a special profile lathe tool, the dimensions of which were checked periodically on a profilometer. Care was also taken to eliminate any transverse scratches in the notches by spinning the test pieces in a lathe between centers and polishing the notches with a fine emery thread. The radius of the thread was less than the radius of the notch. The thread was moved in such a direction that it removed the circumferential scratches and left only very faint axial scratches. The dimensions of the finished specimens were measured to four significant figures on the profilometer.

Notched fatigue specimens were used in place of uniform specimens in order to locate accurately the failure position both in the fatigue and in the slow-bend tests. Additional unnotched specimens were also tested to establish the unnotched S-N curves.

APPARATUS

The fatigue tests were conducted in standard commercial fatigue machines of the R. R. Moore type at a speed of 10,000 rpm.

Slow-bend tests at constant deflection rates and temperatures were employed to determine the effects of the prior cycles of fatigue stressing on the mechanical properties. The testing equipment is designed to load a specimen in simple bending at a constant speed and temperature and to supply a load-deflection record of the test. Type AB 7 SR-4 electric strain gages connected in a bridge circuit are used to measure both the load and the deflection. The integral parts of the apparatus include the loading machine with strain gages, a thermocouple and millivoltmeter, a stop watch, electronic recorder, and still camera. The over-all picture of the test cabinet and electronic recorder is shown in figure 4. Figure 5 depicts the loading equipment and the electronic-recorder panel connections are illustrated in figure 6.

The loading device is a lever system which transmits the load to the specimen resting on a suitable support. The support, specimen, and electric strain gages are housed in an Aminco Sub-zero Test Cabinet. The cabinet can be cooled to -100° F by forced circulation of dry ice, and the specimen can be further cooled by pouring liquid nitrogen around it.

The time of testing is measured either by the Z-axis of the electronic recorder which places a "dot" on the load-deflection record at regular time intervals, or by a stop watch at the slower speeds.

An alternating-current bridge system is employed whereby a 5500-cycle-per-second voltage is introduced into the load bridge and the deflection bridge with the resulting unbalance from loading or deflecting detected, amplified, and transmitted to a 5LP1 tube. A record is made with a still camera. The load bridge and the deflection bridge contain a type AB 7 SR-4 strain gage in each of the four arms.

TESTING PROCEDURE

Specimens of all three materials were subjected to different numbers of prior fatigue cycles both below and above the fatigue limits. They

were then subjected to slow-bend tests in the apparatus described above. In order to determine a brittle transition temperature (where it occurred), the general procedure was as follows. A pilot specimen was first tested in slow-bend at a constant deflection rate and at some estimated constant temperature. If the load-deflection curve showed a departure from linearity, indicating the presence of some macroscopic plastic flow, the same specimen was retested at the same deflection rate but at a lower temperature. This was repeated until the load-deflection record showed a straight line to fracture. Then since the pilot specimen contained a certain amount of cold-work, virgin specimens were tested at the same deflection rate but at temperatures bracketing the one determined above until the transition temperature was pinned down to within $\pm 2^{\circ}$ F. The transition temperature so determined is defined as the highest temperature for a given constraint (triaxiality) and strain rate at which all macroscopic plastic flow ceases. This procedure was applied to the SAE 4130 steel which showed definite transition temperatures.

A different method was employed for the aluminum alloys which did not show transition temperatures within the temperature and velocity limitations of the apparatus. In order to evaluate the effect of prior cycles of fatigue on these alloys, the energy required to fracture at a given deflection rate (0.015 in./sec) and testing temperature (-320° F and 0° F) was selected as a basis of evaluation. The deflection rate was chosen the same for all metals. The reason for selecting the temperature of -320° F as the testing temperature (instead of room temperature) was to bring out the most drastic differences between the aluminum alloys. Tests were also included at 0° F for comparison.

In addition to measuring the changes in mechanical properties of the specimens due to cyclic loading extensive micrographic studies were undertaken to observe and measure crack formation and propagation. Specimens were stressed to various numbers of cycles and removed from the fatigue machine, sectioned longitudinally, metallographically polished (and etched if necessary), and examined under magnification.

Additional special tests were included such as Charpy impact tests, microhardness surveys, tension tests on notched and unnotched specimens, fretting-corrosion tests, and so forth to bring out further certain specific differences in the mechanical behavior of the various materials tested. Also several dye penetrants were tried in an effort to aid in the detection of surface cracks.

EFFECT OF NOTCHES ON ENDURANCE PROPERTIES

The S-N curves for completely reversed bending were first established for the three materials tested in the as-received condition. Three

specimen shapes were tested as illustrated in figure 3, namely, the uniform specimen, the U-notched specimen having a notch 1/16 inch deep with a 1/16-inch radius, and the V-notched specimen having a notch 1/16 inch deep with a radius of 0.01 inch at the bottom and a 45° included angle. The results are shown in figure 7. A comparison of the theoretical with the fatigue stress-concentration factors is given in table II. The number of cycles for which the stress-concentration factors were determined was 10,000,000 for the steel and 100,000,000 for the aluminum alloys.

CRACK STUDIES

In previous studies by the authors (reference 1) it was found that substantial increases occurred in the transition temperature of SAE 1020 steel after subjecting specimens to prior cycles of fatigue short of failure. This occurred at stress levels both above and below the notched endurance limit. In reference 1 various tentative explanations were suggested to account for this phenomenon. In a further development using a different approach in testing technique Lessells and Jacques (reference 2) demonstrated the presence of small cracks in specimens subjected to prior fatigue cycles both above and below the notched endurance limit on two similar low-carbon steels. An explanation of why the cracks on specimens stressed below the notched endurance limit did not continue to ultimate failure, based upon rate of crack growth, was suggested in a subsequent paper (reference 3). Since these low-carbon steels showed increases in transition temperature at the same time, it was considered that this could be accounted for by the origin and growth of these small cracks.

It was deemed important, therefore, to determine whether this was a peculiarity of mild steel or whether this phenomenon occurred in other metals as well. Consequently, crack studies were made of specimens subjected to prior fatigue cycles for all three of the metals discussed here for stresses below and above the endurance limits. The technique used was described earlier under "Testing Procedure." Figures 8 to 10 show typical longitudinal sections revealing fatigue cracks for the three metals stressed above the notched endurance limit for different numbers of cycles. Figures 8(a) to 8(c) are for V-notched specimens; figures 9(a) and 9(b), for U-notched specimens; and figures 10(a) and 10(b), for unnotched bars. This method yielded erratic results because the circumferential cracks which originated at the root of the notch and penetrated radially inward were not necessarily symmetrical about the axis of rotation of the specimens. Thus, it was found satisfactory to photograph the stressed and subsequently fractured specimens which showed two clearly distinguishable areas, an outer ring due to the slowly penetrating cumulative "cracks" and the inner "core" which was suddenly fractured. Figures 11

and 12 illustrate such typical photographs. Figures 11(a) to 11(c) refer to sharp V notches and figures 12(a) to 12(c) refer to U notches. A plot of average crack depth, obtained by the latter method, against the number of cycles for the three metals for particular prior stress levels is included in figure 13.

Sufficient time was not available to study nondestructive methods of crack detection to any appreciable extent. X-ray methods did not appear promising. Sperry Products, Inc., contacted by Professor Carl F. Floe, did not feel that supersonic procedures would be fruitful on notched specimens of the type used. Consequently, no further work was carried out on this problem.

It should be clearly stated, however, that with the present technique of sectioning for crack detection the three metals tested did not show any cracks when stressed below their notched endurance limits. Tests were made on specimens previously stressed at various fractions of the notched endurance limits and carried out to 50×10^6 cycles without any evidence of the formation of cracks. This behavior then was apparently different from that shown by the low-carbon steels previously tested. It is still possible that a more refined technique might reveal minute cracks for this range.

CHANGE IN TRANSITION TEMPERATURE OF SAE 4130 STEEL DUE TO CYCLIC STRESSING

The SAE 4130 steel when subjected to prior cycles of stress above the notched endurance limit showed a steady increase in transition temperature with prior cycles. Table III provides the numerical data for figure 14. Figure 14(a) shows the transition temperature plotted against the number of prior cycles for sharp V-notched specimens, including the rate of change of transition temperature with cycles. The prior stress level was 33,000 psi. It is seen that the transition temperature increased to room temperature at the end of its fatigue life. The rate of change of transition temperature continuously decreased with prior cycles. The U-notched specimens (fig. 14(b)), subjected to prior fatigue stress levels of 46,000 psi (which gave a life of 450,000 cycles, about the same as for the V-notched specimens at a stress level of 33,000 psi), showed a similar increase in transition temperature with prior cycles, although it required about 200,000 cycles before much change took place. After this, the rate of change of transition temperature for the next 200,000 cycles was about the same as that for the first 200,000 cycles for the V-notched specimens.

Previous studies (references 1 and 3) of the effect of prior cycles above the notched endurance limit for SAE 1020 steel showed that the transition temperature also increased toward room temperature for V-notched specimens.

Transition-temperature studies for specimens stressed below the notched endurance limit did not reveal any important changes for this material.

COMPARISON OF ENERGIES ABSORBED IN SLOW-BEND FOR 24S-T4 AND 75S-T6

The difference in behavior of the two aluminum alloys for the V notch is shown in figure 15(a) where the average energy to fracture at -320° F and at an average deflection rate of 0.015 inch per second is plotted against the percent of life. The prior fatigue stress level for the 24S-T4 was 13,000 psi and for the 75S-T6, 15,000 psi. It can be seen that for any number of cycles of fatigue, the 75S-T6 absorbs considerably less energy to fracture than the 24S-T4. While a slightly higher fatigue stress level was employed for the 75S-T6, it can be noted that the greatest difference in the energy-absorption capacity between these two metals is for no prior fatigue stressing, thus indicating that the slight difference in stress levels did not account for the effect.

The low temperature of -320° F was chosen for the above tests in order to emphasize any difference between the two aluminum alloys. It was considered desirable, however, to repeat the tests for the same V-notched specimens but for fracture in slow-bend at a temperature closer to service conditions. Consequently, figure 15(b) shows the average energy to fracture for both alloys plotted against percent life at the same average deflection rate when tested at 0° F. It was found that the endurance properties changed from bar to bar sufficiently that in order to secure failure within 450,000 to 500,000 cycles it was necessary to raise the fatigue stress level for 24S-T4 to 16,000 psi. Thus the conditions as far as stress level is concerned are not strictly comparable. An examination of figure 15(b) discloses that the energy absorbed decreased with increasing number of cycles as before but the 75S-T6 now absorbs more energy to fracture than the 24S-T4. It is felt that the change in order of magnitude of energy absorbed between the two alloys is (for no prior cycles) due to the difference in mechanical properties in the as-received condition from bar to bar and to the change in testing temperature. It can be further noted from figures 15(a) and 15(b) that the 75S-T6 showed more scatter and less reproducibility

than the 24S-T4. This is not surprising since the harder the material, the greater will be the scatter in the results.

EFFECT OF NOTCH GEOMETRY ON ENERGY ABSORBED IN 24S-T4 AND 75S-T6 ALLOYS

Specimens of 75S-T6 and 24S-T4 were prepared with a U notch having the same depth as the V notch but a radius of 1/16 inch as shown in figure 3. These were subjected to fatigue stress levels of 26,000 psi for the 24S-T4 and 25,000 psi for the 75S-T6 so selected as to produce failure in about 450,000 cycles. The energies absorbed in slow-bend at -320° F are plotted in figure 16 against percent life. It can be concluded from this figure that:

(1) The sharpness of the notch effects a much greater percentage reduction in energy absorbed for the 75S-T6 as compared with the 24S-T4 (cf. figs. 15(a) and 16). This indicates greater notch sensitivity for the 75S-T6.

(2) The scatter is much larger with increased radius of notch.

(3) A higher notch fatigue stress is required for the 24S-T4 than for the 75S-T6 to produce failure for the same number of cycles.

EFFECT OF HEAT TREATMENT ON ENERGY ABSORBED FOR 75S-T6 AND 24S-T4

Tests to determine the mechanical properties of 24S-T4 and 75S-T6 in the as-received condition, as shown in table IV, revealed that the 75S-T6 had a Rockwell B hardness of 88 as compared with a Rockwell B of 76 for the 24S-T4. The tensile properties also indicated that the 75S-T6 was stronger and less ductile than the 24S-T4. It was felt that the differences in energy absorption previously discussed were probably due to the differences in the above basic properties and attempts were therefore made to re-heat-treat these alloys to produce nearly the same hardness levels. The 75S-T6 specimens were reaged at 350° F for 8 hours. This resulted in a Rockwell B hardness of 76, the same as that of the original 24S-T4. It was not found possible to harden the 24S-T4 specimens to the -T6 level, the maximum hardness of the 24S-T4 obtained being Rockwell B of 84. This was secured by aging at 350° F for 24 hours.

The specimens used were V-notched and tested at -320° F in slow-bend. The stress levels to give a life of about 450,000 cycles were found to be 14,000 psi for 24S-T4 and 13,500 psi for 75S-T6, which are quite close. Figure 17 shows the average energy absorbed plotted against the percent life and compared with the results previously shown in figure 15(a) for the metals as received. The upper two curves show (except for some differences after fatigue stressing up to 20 percent of life) that the energy absorbed is about the same for the reaged 75S-T6 and the original 24S-T4. Somewhat similar results were obtained as shown for reaging the 24S-T4 (to obtain a higher hardness) compared with the original as-received 75S-T6. It may be concluded then that the differences in original hardness levels are largely responsible for the differences shown in energy-absorption capacity.

SPECIAL TESTS

In order to bring out further the differences in mechanical behavior of the two aluminum alloys several special tests were made. These included Charpy impact tests, tension tests, microhardness surveys, and fretting-corrosion tests.

Charpy Impact Test

Figure 18 shows the energy absorbed in Charpy impact for the V-notched specimens plotted against the testing temperatures for both aluminum alloys. It is seen that the 75S-T6 absorbs considerably less energy at all temperatures than the 24S-T4.

The appearance of the fractures in these tests was quite different for the two alloys. Figure 19 shows that at all temperatures the 24S-T4 showed perpendicular cleavage-type fractures. The 75S-T6, on the other hand, at very low temperatures displaced a slanting fracture surface (approximately 45° to the axis) which became a jagged Z-shaped fracture at higher temperatures.

Tension Tests

True stress-strain tension tests at room temperature on unnotched specimens indicated an energy absorption for the 24S-T4 of about six times that for the 75S-T6 in the as-received condition.

Microhardness Surveys

A microhardness survey with the Tukon tester made on V-notched specimens, fatigued for 100,000 cycles and sectioned longitudinally, showed as illustrated in figure 20 that the hardness within 0.002 inch of the notch bottom was somewhat less than the original matrix. It then increased for a depth of about 0.02 inch and leveled off to the hardness of the matrix.

Fretting Corrosion

In conducting the rotating-beam fatigue tests for the current investigation certain anomalous failures occurred. Although three metals were being tested (24S-T4 and 75S-T6 aluminum and SAE 4130 steel) these unexpected failures were confined in the as-received condition to the 75S-T6 aluminum specimens alone. Expected failures occurred at the reduced section of the specimens (notched or unnotched), where the nominal stress is the greatest. In the anomalous failures, the specimens fractured in the collet at the line where contact between collet and specimen is first established. Upon closer examination of these failures a ring of irregular pits and discoloration was observed. Fracture originated from this line, radially inward. Similar damage was observed on most specimens tested in fatigue (for all three materials), especially those which were subjected to stressing close to or below the endurance strength. Such damage was first reported by Eden, Rose, and Cunningham (reference 4). This phenomenon has been described since under several names, the most commonly accepted being fretting corrosion. Its significance in the present investigation is that it caused unpredictable failure in the 75S-T6 only.

Figures 21 to 25 depict typical fretting-corrosion damage on various specimens. Figure 21 shows fretted unnotched specimens of 75S-T6 in the as-received condition where fretting leads to fatigue failure. Figure 22 illustrates a similar failure for a notched specimen of 75S-T6. Figure 23 portrays a 24S-T4 specimen in the as-received condition on which fretting occurred but did not lead to fatigue failure. Figure 24 pictures 24S-T4 specimens artificially aged to approximately the same hardness level as that of the original 75S-T6 material showing fretting corrosion leading to fatigue failure. A 75S-T6 unnotched aluminum specimen, which was heat-treated to reduce its hardness to the level of the 24S-T4 in the as-received condition, fretted in the chuck causing fracture as shown in figure 25.

These fretting-corrosion studies emphasize the much higher degree of notch sensitivity of the 75S-T6 as compared with 24S-T4 as indicated by the results of previous tests discussed earlier.

About 300 fatigue specimens each of 24S-T4 and 75S-T6 aluminum and SAE 4130 steel have been tested during the course of this investigation. Fretting corrosion was evident on most specimens. Those specimens which were drawn into their tapered chucks tightly had less tendency to fret. Specimens run at high stress levels (consequently for a short number of cycles and length of time) likewise exhibit less or even no attack. Three failures originating in the region of the fretting damage occurred in the original 75S-T6 batch. Furthermore, these three specimens were subjected to long-time, low-stress fatigue testing. It is of interest that one specimen had no external notch machined in it (polished, tapered specimen), another had a 1/16-inch-deep, 0.01-inch-radius notch, and the third one so failing had a 1/16-inch-deep, 1/16-inch-radius notch.

When an attempt was made to determine the fatigue stress-concentration factor for the reaged specimens as described above, fretting failures took place in the bearing surfaces leading to actual fatigue fracture at the enlarged ends rather than in the reduced section.

SUMMARY OF RESULTS

Three aircraft metals, namely, SAE 4130 steel and 24S-T4 and 75S-T6 aluminum alloys, were subjected to cyclic loading followed by various physical tests to show the effects of such cyclic loading on their mechanical behavior and particularly to bring out any difference in behavior between the 24S-T4 and 75S-T6 aluminum alloys. These physical tests included slow-bend tests which determined the effect of prior cycles on the transition temperature to brittle fracture for SAE 4130 steel and on the energy-absorption capacity of the aluminum alloys. Crack studies were made to detect the origin of initial failure. Auxiliary tests such as Charpy impact tests, microhardness surveys, tension tests, and fretting-corrosion studies were made to supplement the slow-bend tests. The results are summarized as follows:

1. As found earlier for SAE 1020 steel, the transition temperatures for SAE 4130 steel, when fatigued above the notched endurance limit, increased rapidly with the number of prior cycles.

2. No evidence of either fatigue cracks or changes in transition temperature was established for cycling below the endurance limit for the SAE 4130.

3. Slow-bend tests on the aluminum alloys conducted on V-notched specimens at -320° F showed considerably less energy absorption for 75S-T6 as compared with 24S-T4.

4. The energy absorbed for both aluminum alloys decreased as the number of cycles increased.

5. A comparison of the energies absorbed for V notches and U notches showed that the sharper the notch, the less the energy absorption, but the reduction was much more pronounced for the 75S-T6 than for the 24S-T4 alloy.

6. Charpy impact tests and tension tests both showed the inferior capacity of the 75S-T6 to absorb energy as compared with 24S-T4 in the as-received condition.

7. Fretting-corrosion studies confirmed the higher notch sensitivity of the 75S-T6.

8. By reaging, the hardness of the two aluminum alloys was made approximately the same, resulting in similar energy-absorption capacities after fatigue.

9. The inferior energy-absorption capacity and notch sensitivity of the 75S-T6 compared with 24S-T4 is considered to be due mainly to its higher hardness level rather than to an inherent property.

Massachusetts Institute of Technology
Cambridge, Mass., August 31, 1951

REFERENCES

1. MacGregor, C. W., and Grossman, N.: Some New Aspects of the Fatigue of Metals Brought Out by Brittle Transition Temperature Tests. The Welding Jour., vol. 27, no. 3, March 1948, pp. 132s-144s.

2. Lessells, J. M., and Jacques, H. E.: Effect of Fatigue on Transition Temperature of Steel. The Welding Jour., vol. 29, no. 2, Feb. 1950, pp. 74s-83s.

3. MacGregor, C. W.: Significance of Transition Temperature in Fatigue. Fatigue and Fracture Conference, M.I.T., June 1950.

4. Eden, E. M., Rose, W. N., and Cunningham, F. L.: Endurance of Metals. Proc. Institution Mech. Eng. (London), vol. 4, Oct. 1911, pp. 839-880.

TABLE I

CHEMICAL ANALYSES AND MECHANICAL PROPERTIES OF MATERIALS TESTED

(a) Aluminum alloys

Cast analysis (percent)													
Alloy	Cu	Fe	Si	Mn	Mg	Zn	Cr	Ti	Pb	Bi	Ni	B	Be
24S-T4	4.70	0.27	0.16	0.69	1.54	0.03	0.06	0.03	0	0	0.01	-	-----
75S-T6	1.62	.17	.11	.01	2.50	5.44	.23	.02	0	0	0	0	0.001
Check analysis (percent)													
24S-T4	4.58	0.38	0.17	----	1.53	0.10	----	0.03	-	-	----	-	-----
75S-T6	1.62	.27	.08	----	2.51	5.42	----	.02	-	-	----	-	-----

Finishing mill fabricating history			
Operation	24S-T4	75S-T6	Remarks
Finish-roll 9/16-in. diam.	X	X	Hot-rolled, coiled
Anneal	X	X	24S-T4: 15 min at 660° F; 75S-T6: 15 min at 780° F; air-cool, reheat 30 min at 450° F
Draw 0.500-in. diameter ± 0.0015 in.	X	X	
Solution-heat-treat	X	X	3/4 hr soak at 915° F
Auto stretch 12 ft + 1/8 in. - 0 in.	X	X	
Artificially age		X	250° F for 24 hrs

Mechanical properties					
Item	Alloy	Sample position	Tensile strength (psi) (1)	Yield strength (psi)	Elongation in 4 diam. (percent) (1)
1	24S-T4	Pieces marked 8-9 and 30-31	70,500	58,000	17.7
2	75S-T6	Piece marked 0-1	83,700	77,400	15.0

[1]Average of three tests.

TABLE I.- Concluded

CHEMICAL ANALYSES AND MECHANICAL PROPERTIES OF MATERIALS TESTED - Concluded

(b) Steel alloy

Ladel analysis (percent)									
Alloy	C	Mn	P	S	Si	Ni	Cr	Mo	Cu
SAE 4130	0.30	0.50	0.004	0.016	0.26	0.18	0.95	0.21	----
Check analysis (percent)									
SAE 4130	0.30	0.47	0.009	0.029	0.28	0.11	0.90	0.22	0.04

Test results
The steel from heat X24709 was processed and tested to meet the requirements of Army-Navy Specification AN-QQ-S-684a: (1) Etch tests on semifinished products taken from the top, middle, and bottom portions of the first, middle, and last two ingots of the heat were good insofar as meeting the requirements of electric aircraft quality steel (2) Magnaflux test, very good (3) Cleanliness test, very good
Heat treatment
Quenched in oil from 1625° F and drawn at 950° F
Mechanical properties

Yield strength	113,850 psi
Tensile strength	130,600 psi
Elongation in 2 in.	25.5 percent
Reduction of area	64.2 percent

TABLE II

THEORETICAL AND FATIGUE STRESS-CONCENTRATION FACTORS FOR NOTCHES EMPLOYED

Material	U-shaped notch		V-shaped notch	
	Theoretical	Fatigue	Theoretical	Fatigue
SAE 4130	1.6	1.42	3.1	2.47
24S-T4	1.6	1.29	3.1	2.22
75S-T6	1.6	1.54	3.1	2.08

TABLE III

TRANSITION-TEMPERATURE VALUES OF SAE 4130 STEEL AFTER VARIOUS PRIOR CYCLES OF FATIGUE STRESSING

Cycles	Transition temperature, T_t (°F)	Rate of change of transition temperature, $\frac{\Delta T_t}{\Delta N} \times 1000$
1/16-in.-deep notch with 0.01-in. radius; 33,000 psi		
0	-245	0
4,000	-221	6.0
10,000	-201	3.33
50,000	-121	2.00
100,000	-13	2.16
200,000	11	.24
300,000	40	.29
400,000	69	.29
1/16-in.-deep notch with 1/16-in. radius; 46,000 psi		
0	-320	----
100,000	-320	0
200,000	-320	0
250,000	-208	2.24
300,000	-170	.76
350,000	-135	.70
400,000	-70	1.30
450,000	-42	.56

TABLE IV

MECHANICAL PROPERTIES OF 24S-T4 AND

75S-T6 ALUMINUM ALLOYS

Alloy	Tensile strength (psi)	Hardness (R_B)	Elongation (percent)
24S-T4	70,500	76	17.7
24S-T4 reaged	73,300	84	11
75S-T6	85,700	88	15
75S-T6 reaged	73,200	76	16

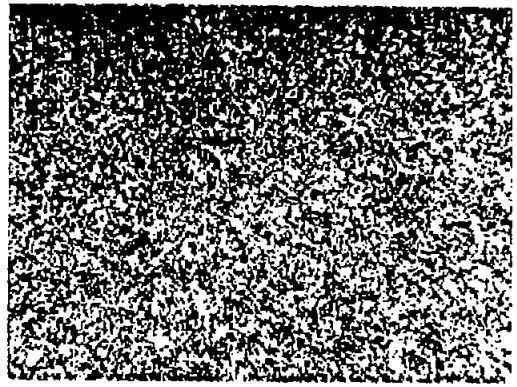

(a) Transverse. X100.

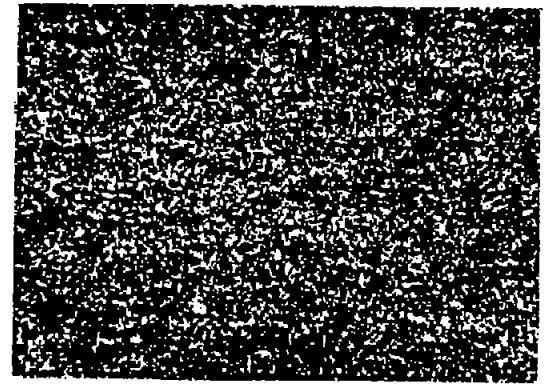

(b) Longitudinal. X100.

(c) Transverse. X500.

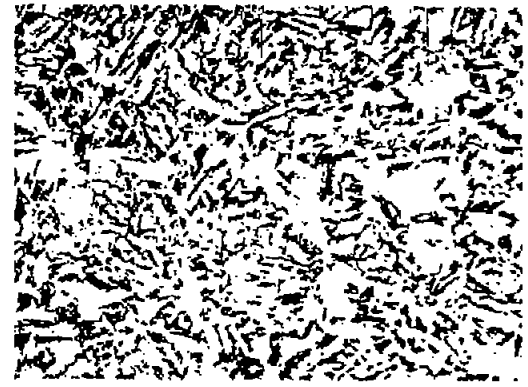

(d) Longitudinal. X500.

Figure 1.- Photomicrographs of SAE 4130 steel tested.

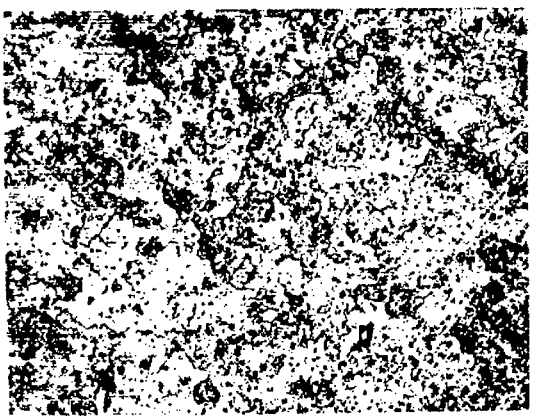

Transverse

Longitudinal

(a) 24S-T4 aluminum alloy as received.

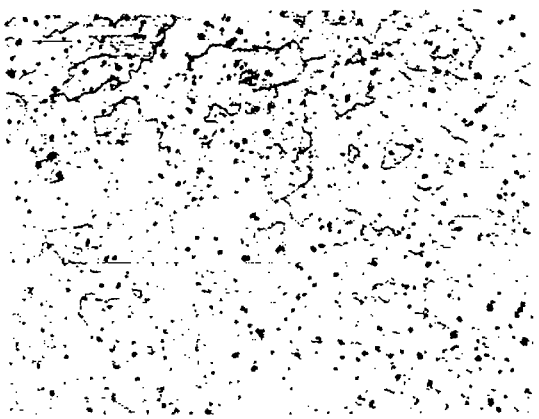

Transverse

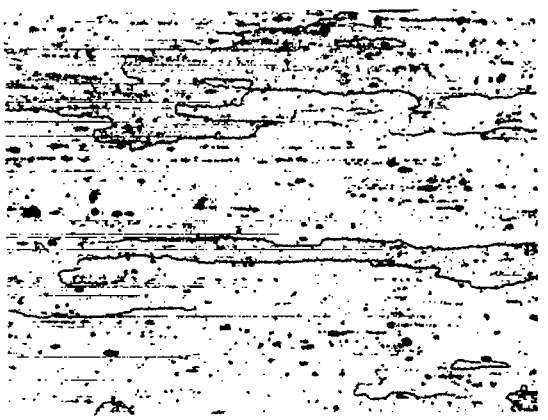

Longitudinal

(b) 75S-T6 aluminum alloy as received.

Figure 2.- Photomicrographs of aluminum alloys tested. X100.

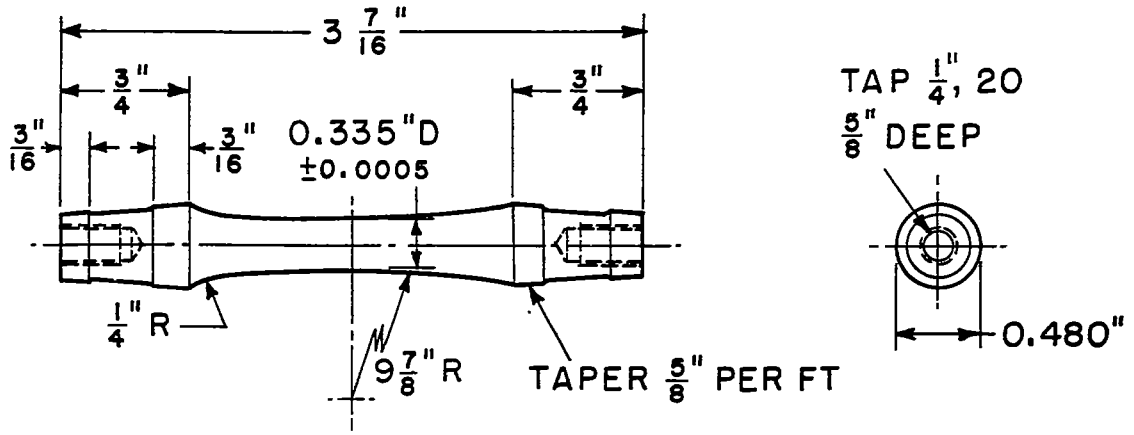

(a) Uniform specimen.

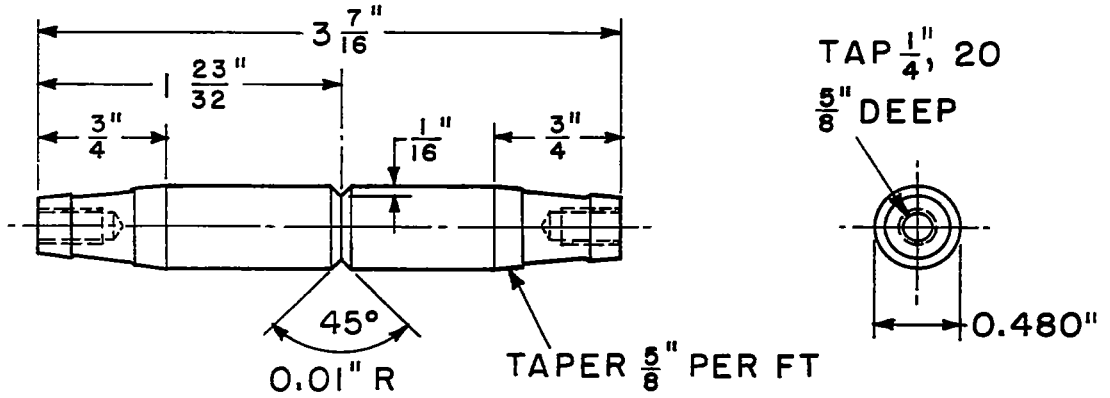

(b) V-notched specimen.

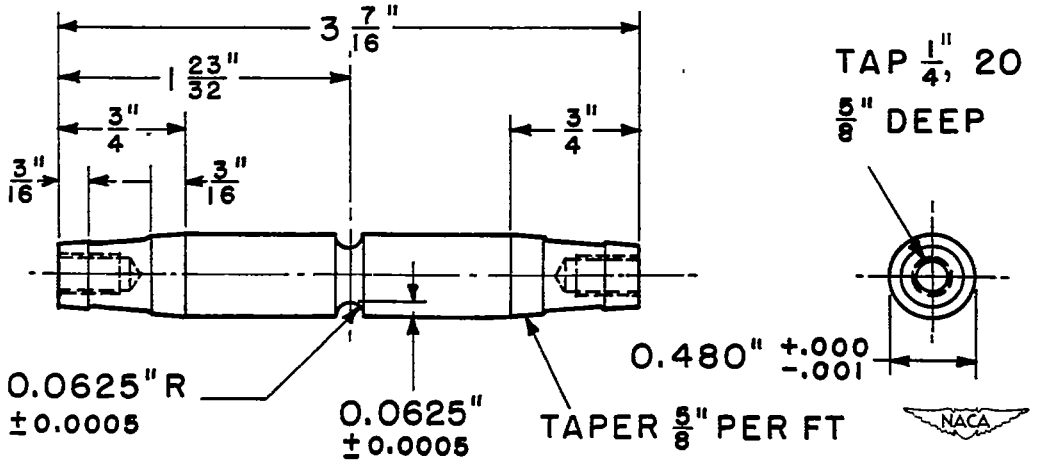

(c) U-notched specimen.

Figure 3.- Dimensions of test specimens.

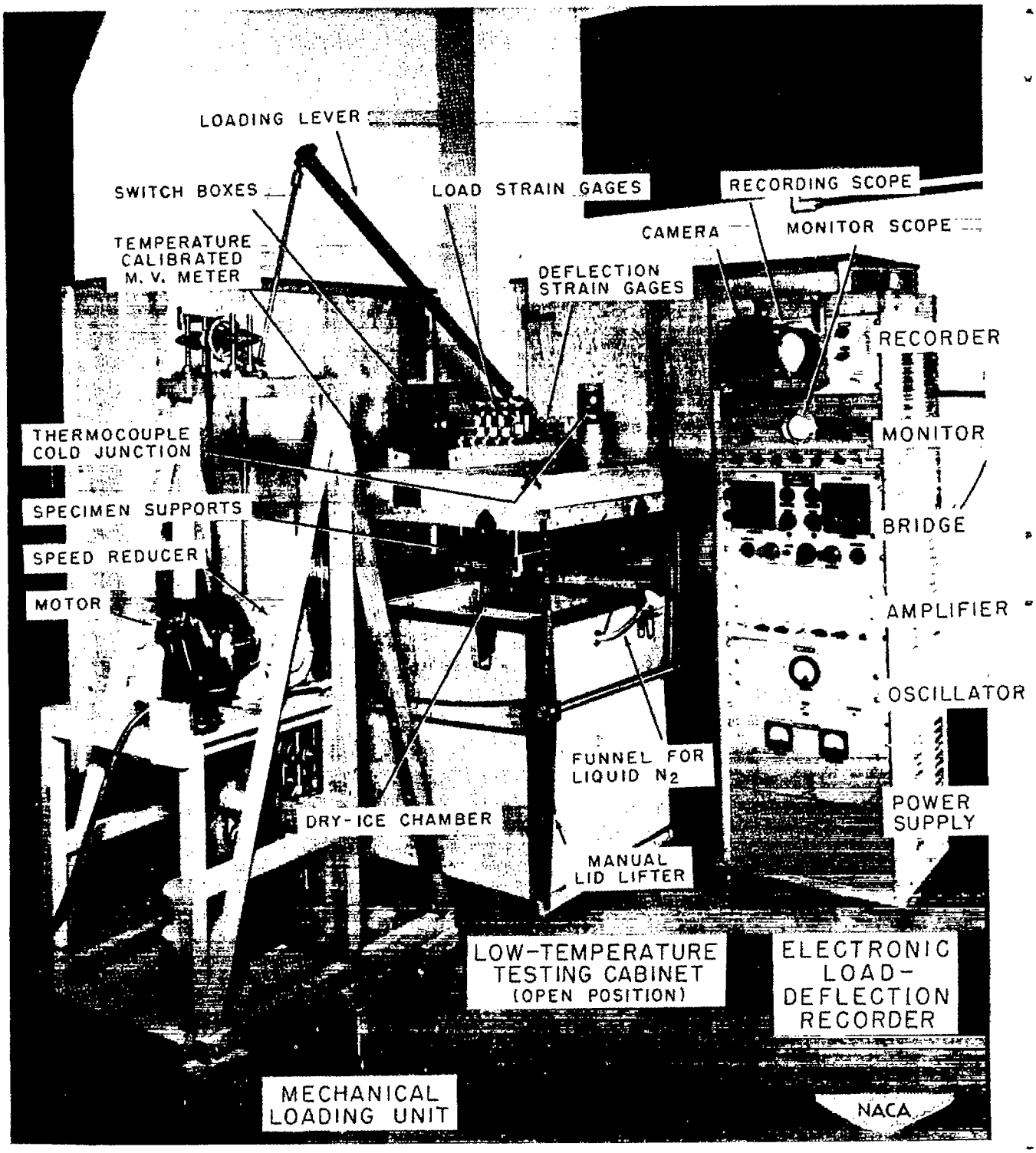

Figure 4.- Slow-bend testing equipment and electronic recorder.

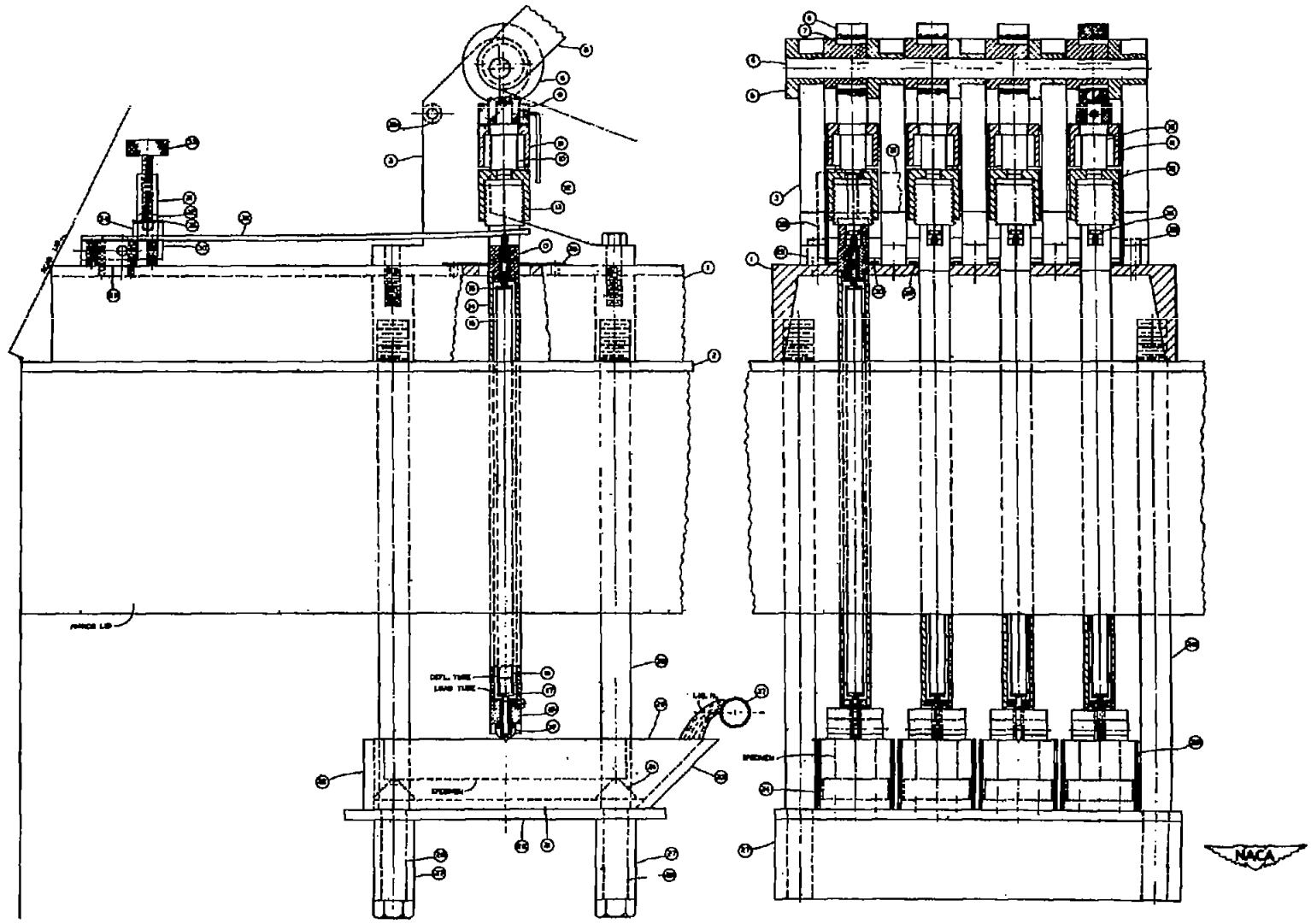

Figure 5.- Loading-equipment assembly drawing.

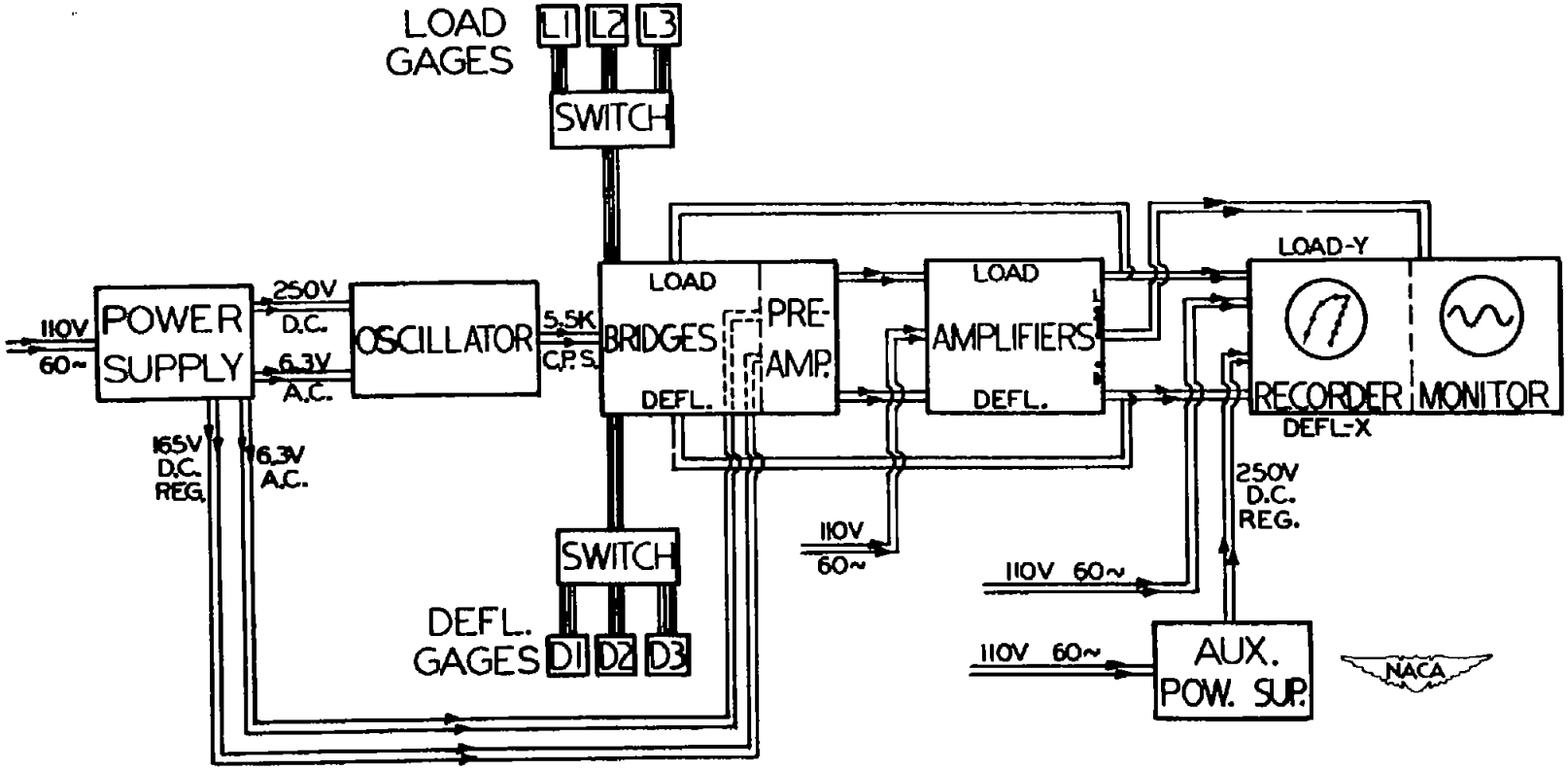

Figure 6.- Panel connections for electronic recorder with alternating-current bridge.

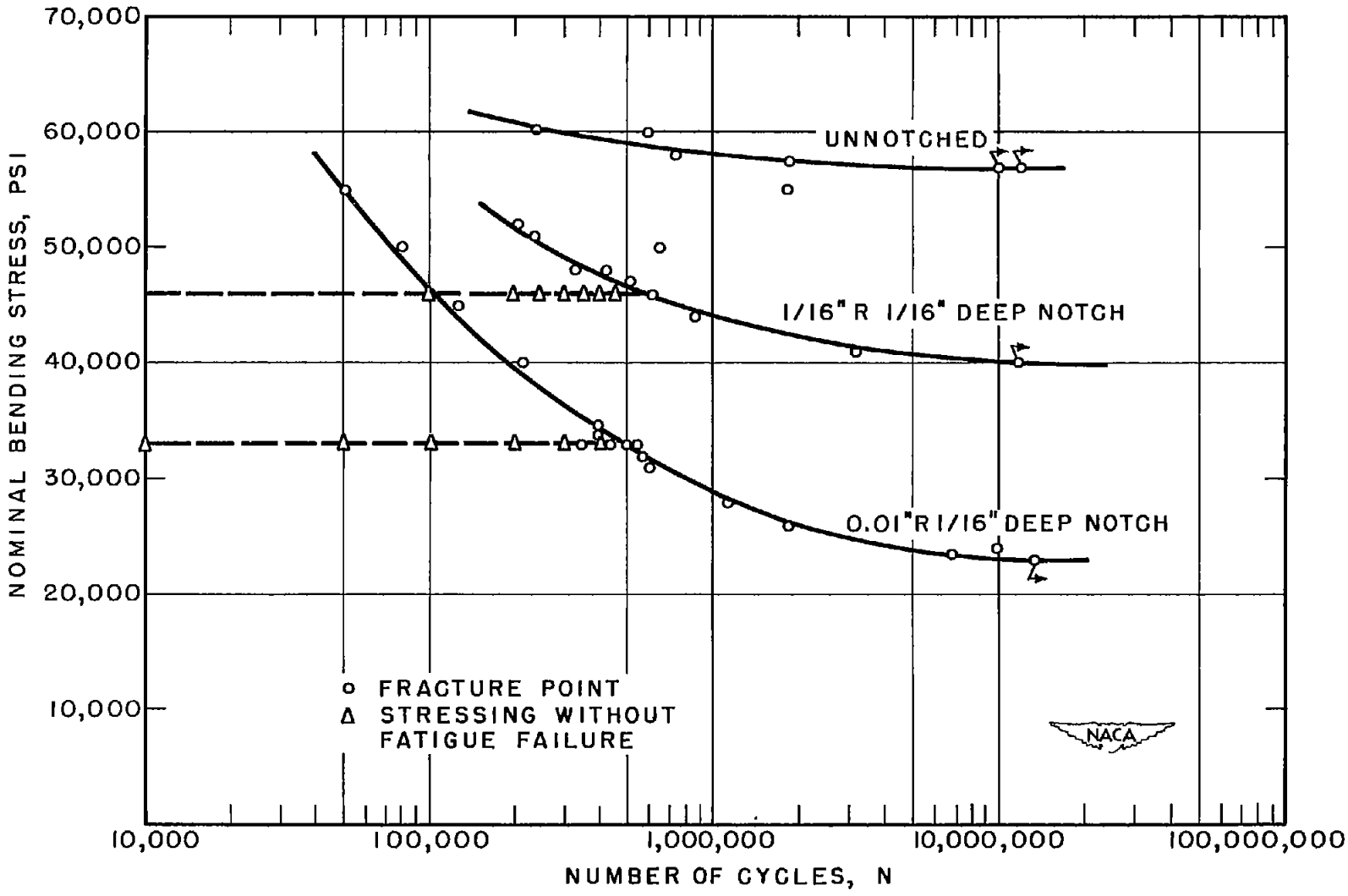

(a) For SAE 4130 steel.

Figure 7.- S-N curves showing location of prior cycles of fatigue for brittle temperature tests.

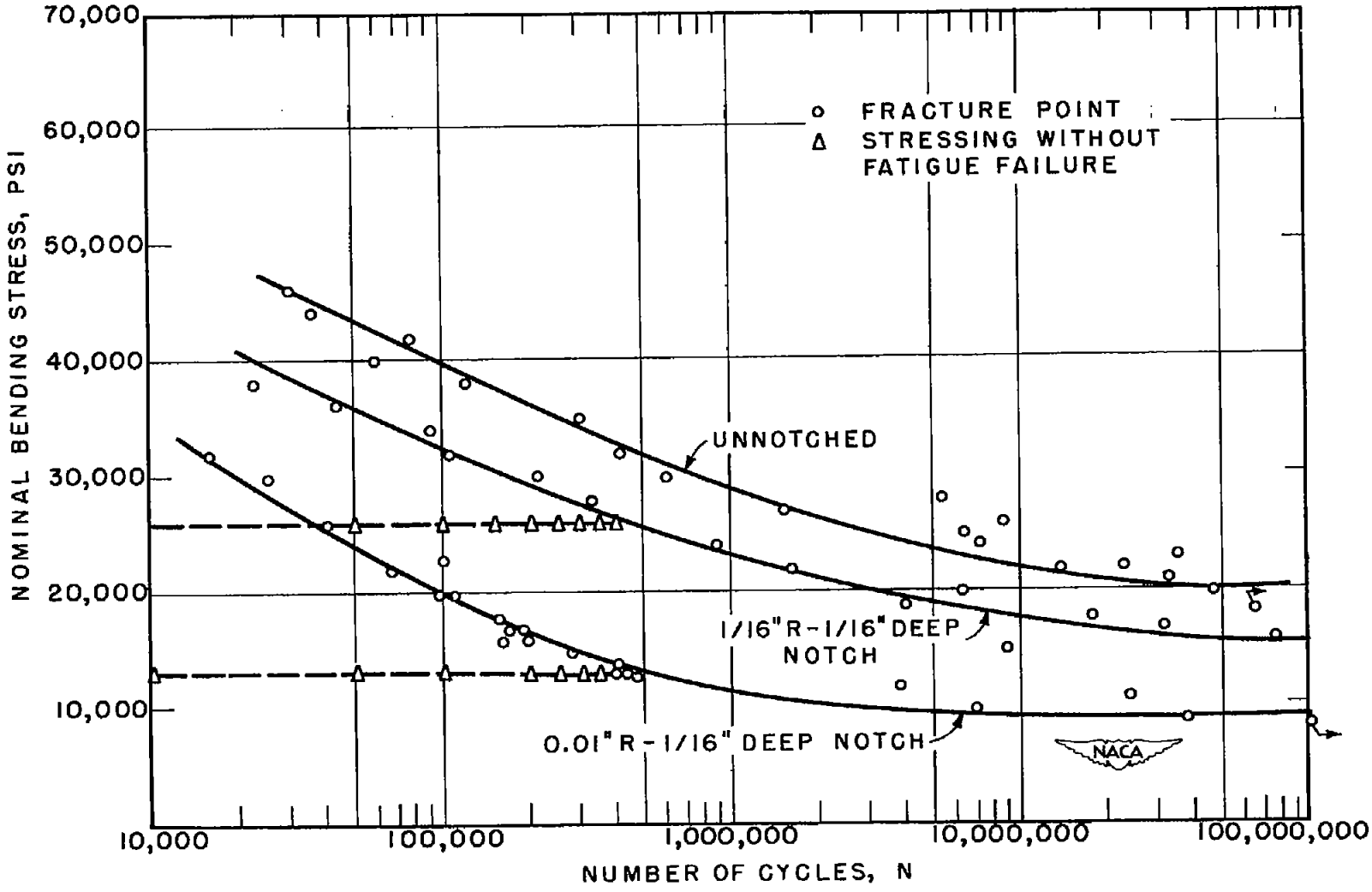

(b) For 24S-T4 aluminum alloy.

Figure 7.- Continued.

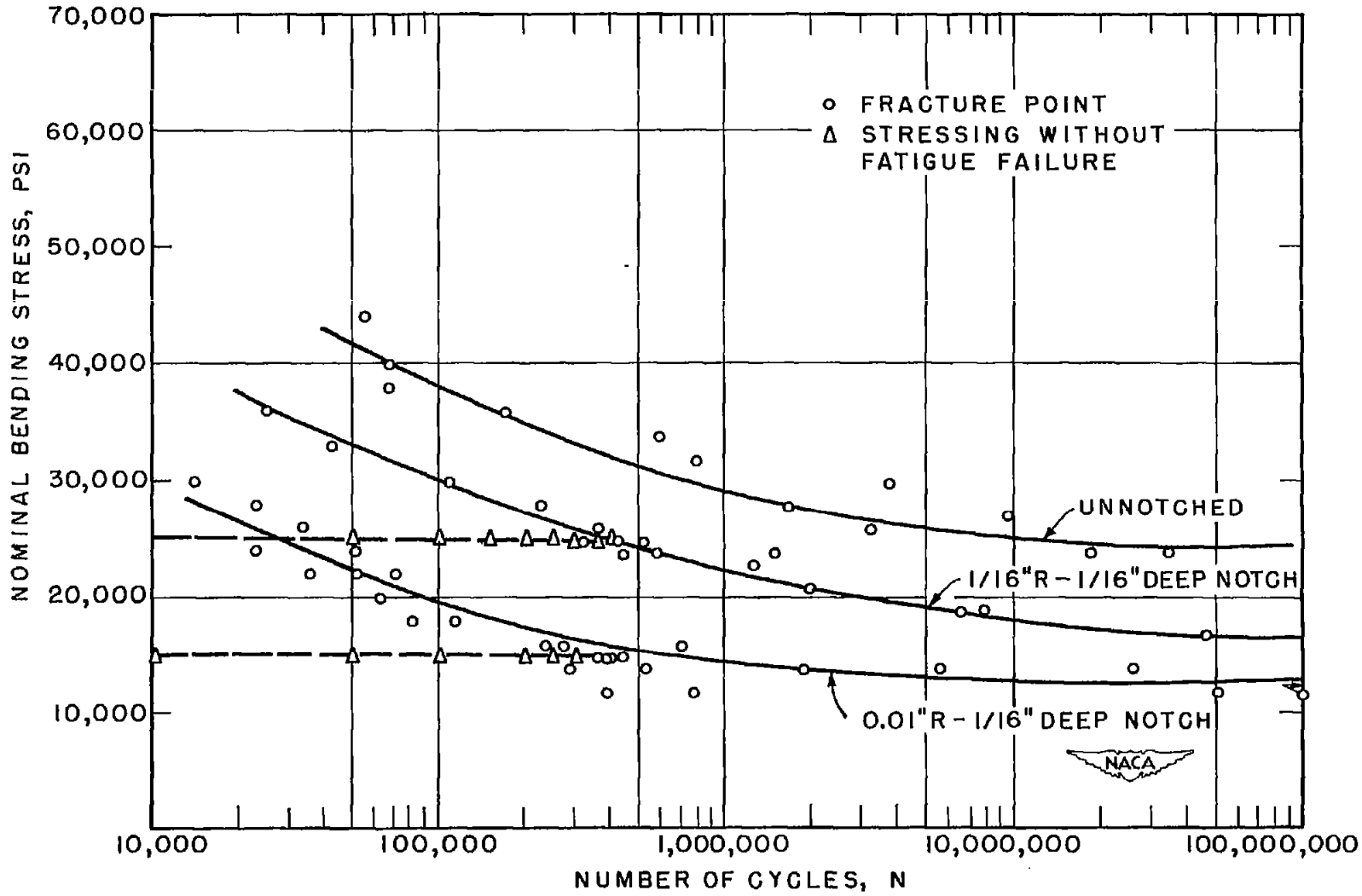

(c) For 75S-T6 aluminum alloy.

Figure 7.- Concluded.

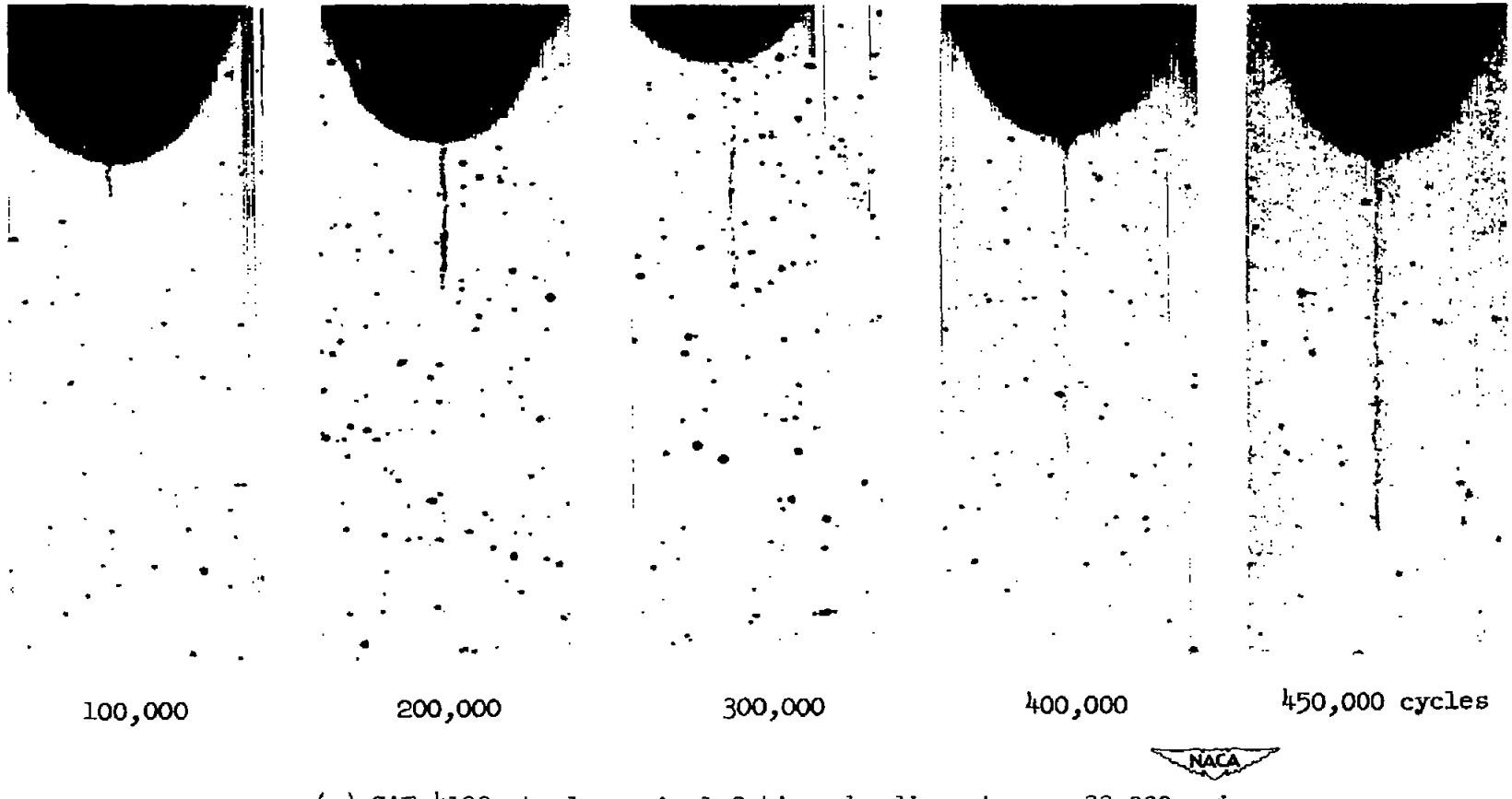

(a) SAE 4130 steel; nominal fatigue bending stress, 33,000 psi.

Figure 8.- Longitudinal sections of V-notched specimens showing cracks after various numbers of cycles of fatigue stressing. Notch, 1/16 inch deep with 0.01-inch radius.

(b) 24S-T4 aluminum alloy; nominal fatigue bending stress, 13,000 psi.

Figure 8.- Continued.

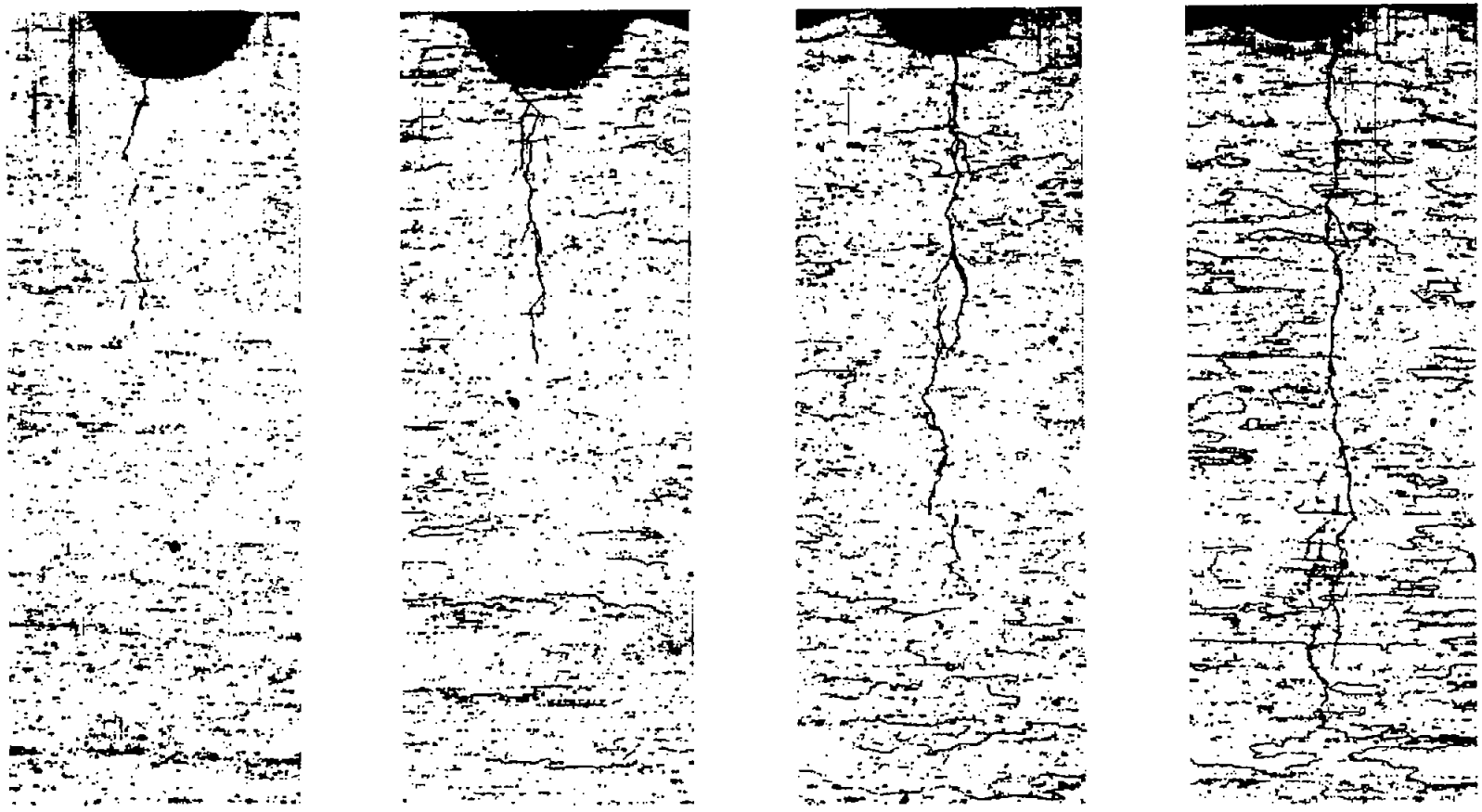

(c) 75S-T6 aluminum alloy; nominal fatigue bending stress, 15,000 psi.

Figure 8.- Concluded.

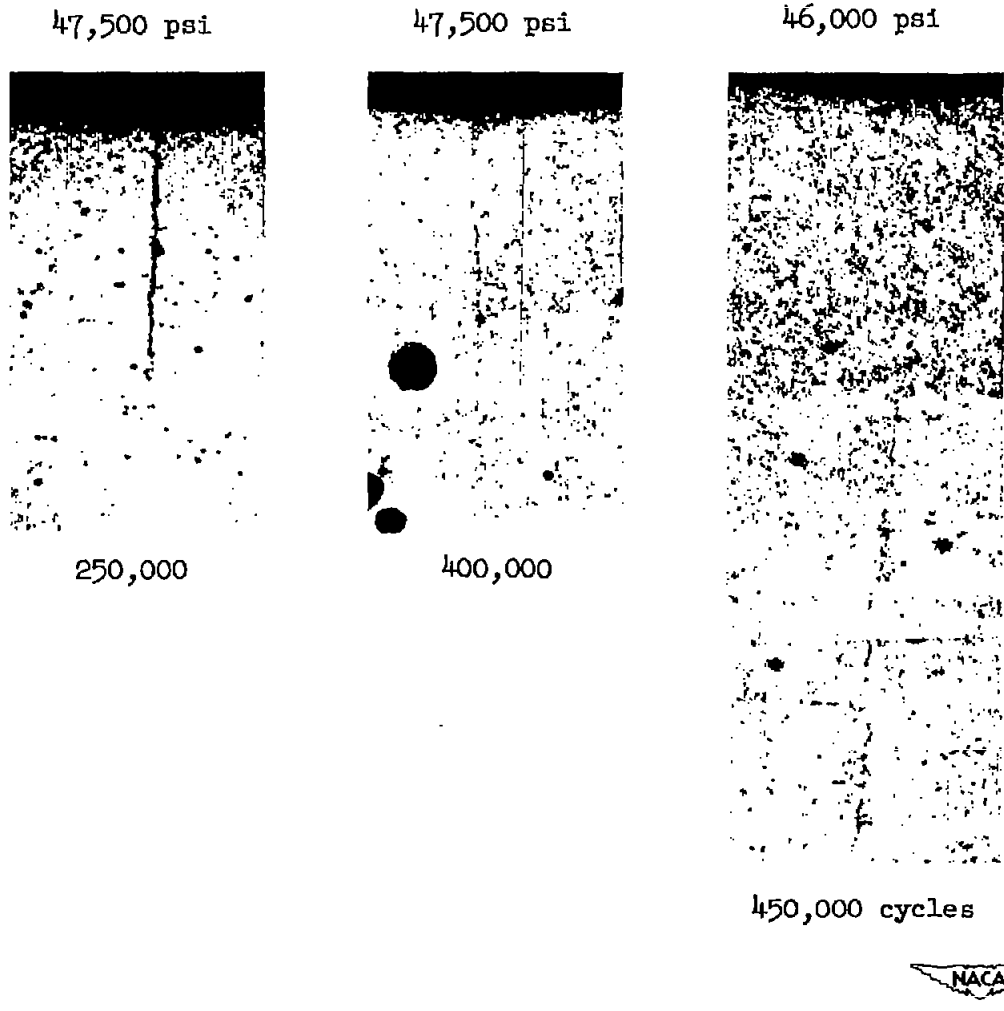

(a) SAE 4130 steel; nominal fatigue bending stresses indicated.

Figure 9.- Longitudinal sections of U-notched specimens showing cracks after various numbers of cycles of fatigue stressing. Notch, 1/16 inch deep with 1/16-inch radius.

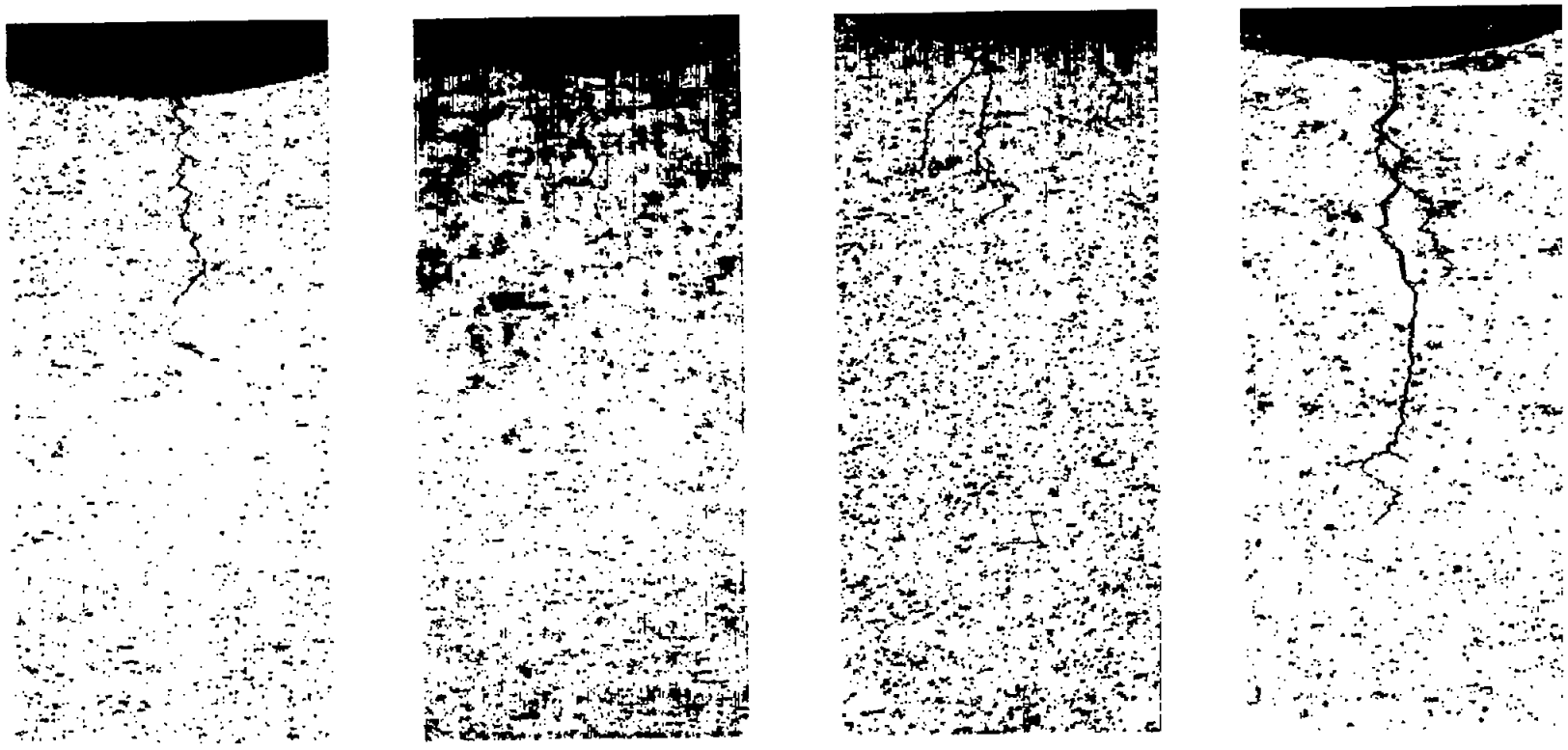

(b) 24S-T4 aluminum alloy; nominal fatigue bending stress, 26,000 psi.

Figure 9.- Concluded.

500,000 400,000 cycles

NACA

(a) SAE 4130 steel; nominal fatigue bending stress, 60,000 psi.

Figure 10.- Longitudinal sections of unnotched specimens showing cracks after various numbers of cycles of fatigue stressing.

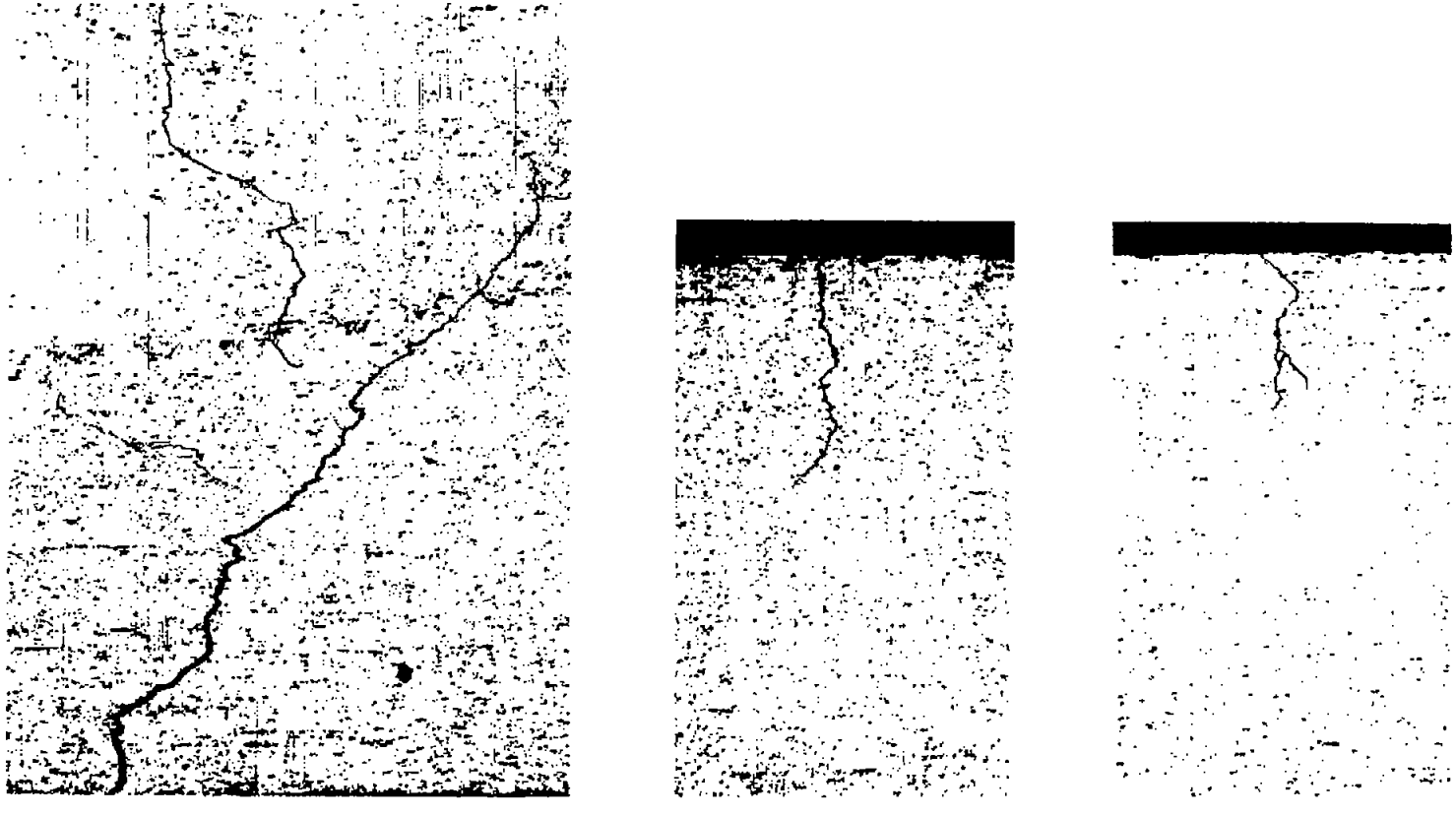

(b) 24S-T4 aluminum alloy; nominal fatigue bending stress, 37,000 psi.

Figure 10.- Concluded.

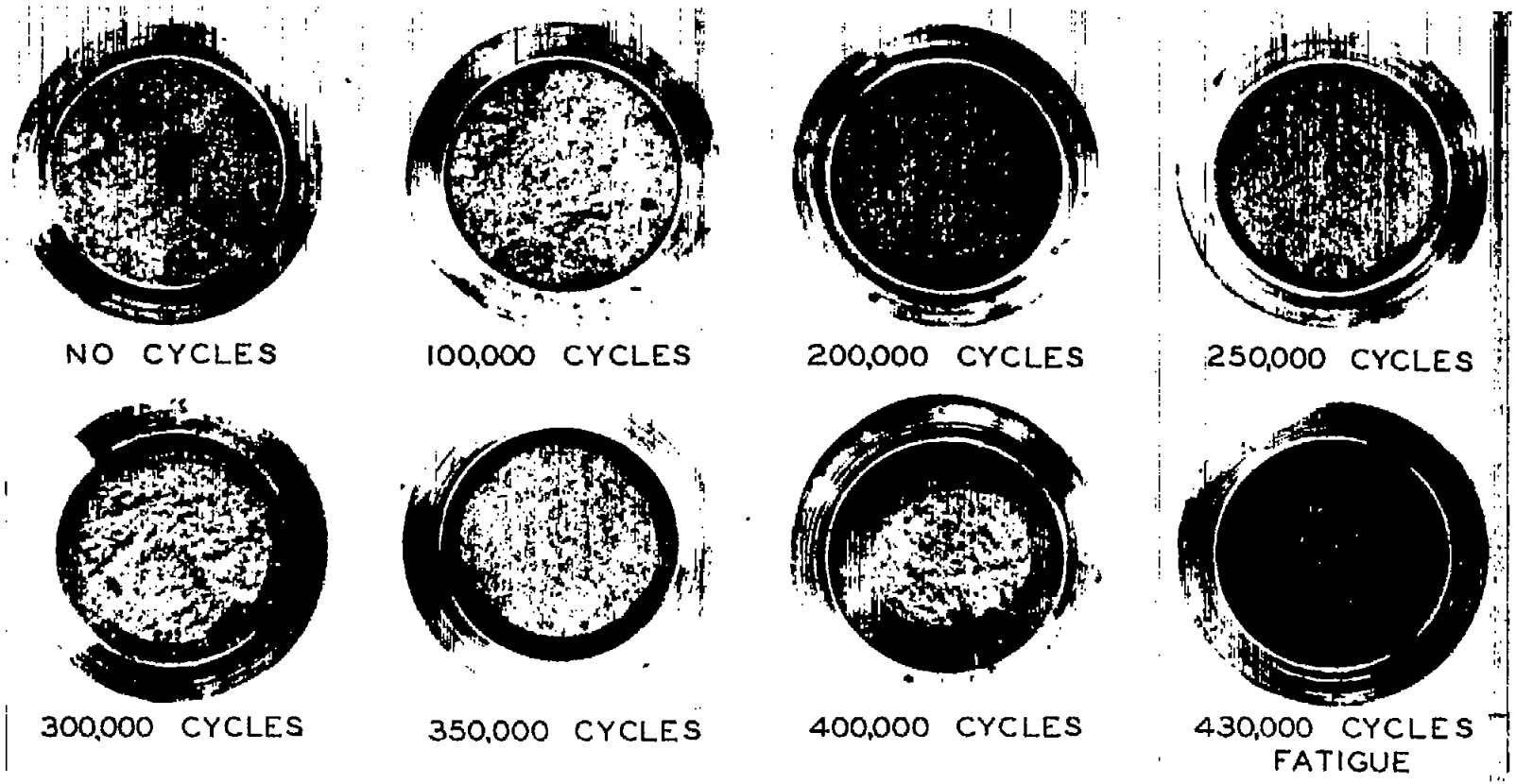

(a) SAE 4130 steel; nominal fatigue bending stress, 33,000 psi.

Figure 11.- Typical views of slow-bend fractures of V-notched specimens after various cycles of fatigue stressing. Notch, 1/16 inch deep with 0.01-inch radius.

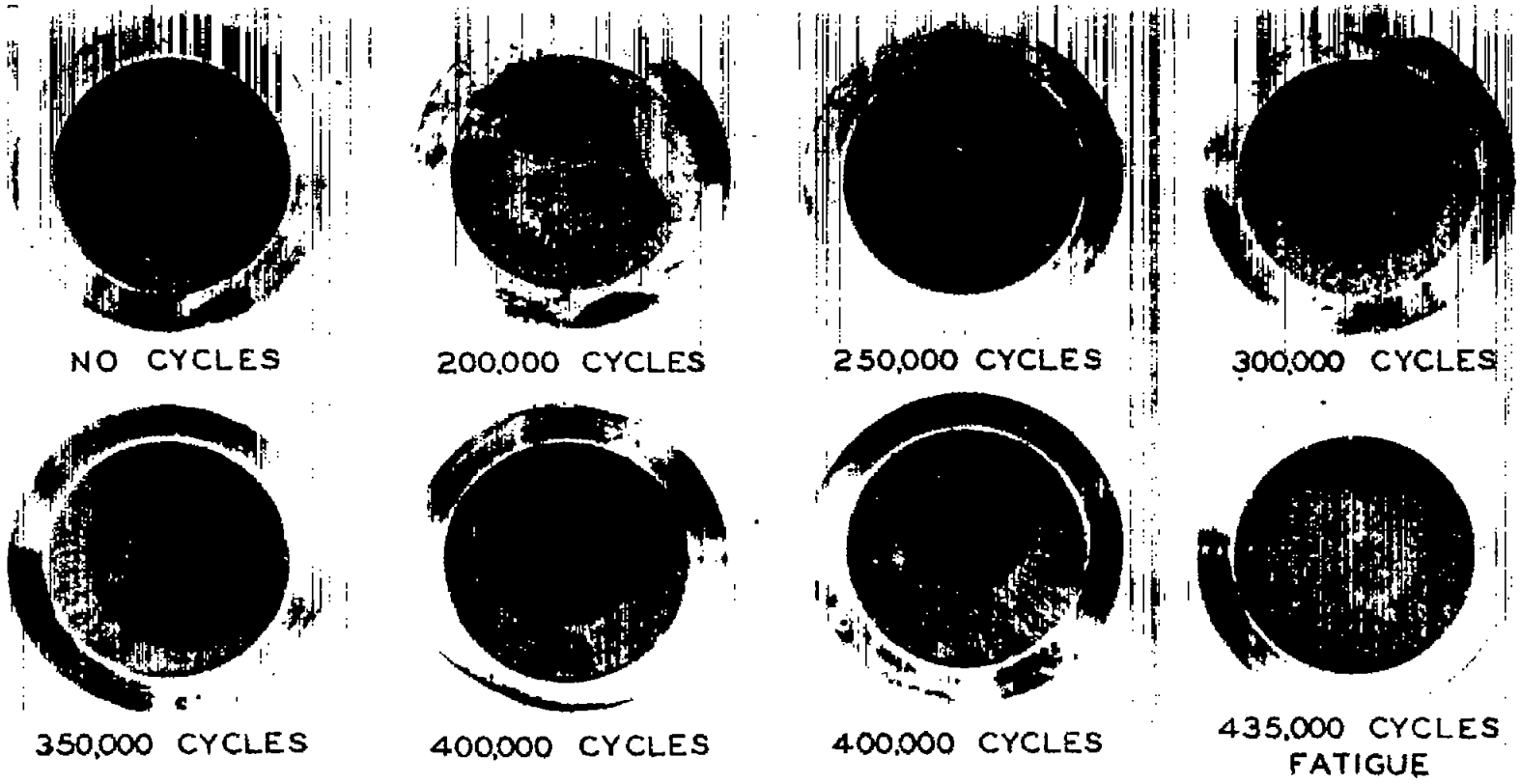

(b) 24S-T4 aluminum alloy; nominal fatigue bending stress, 13,000 psi.

Figure 11.- Continued.

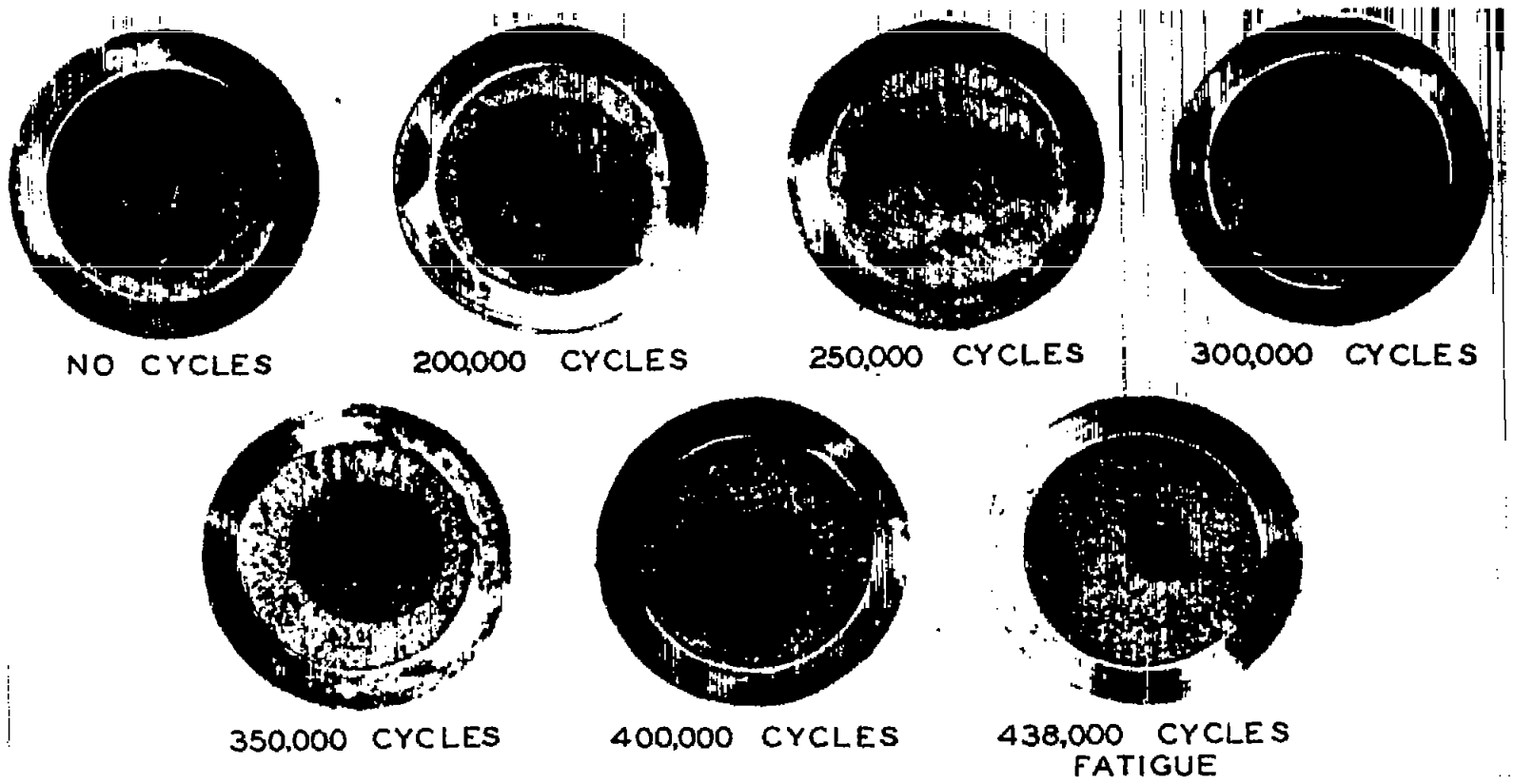

(c) 75S-T6 aluminum alloy; nominal fatigue bending stress, 15,000 psi.

Figure 11.- Concluded.

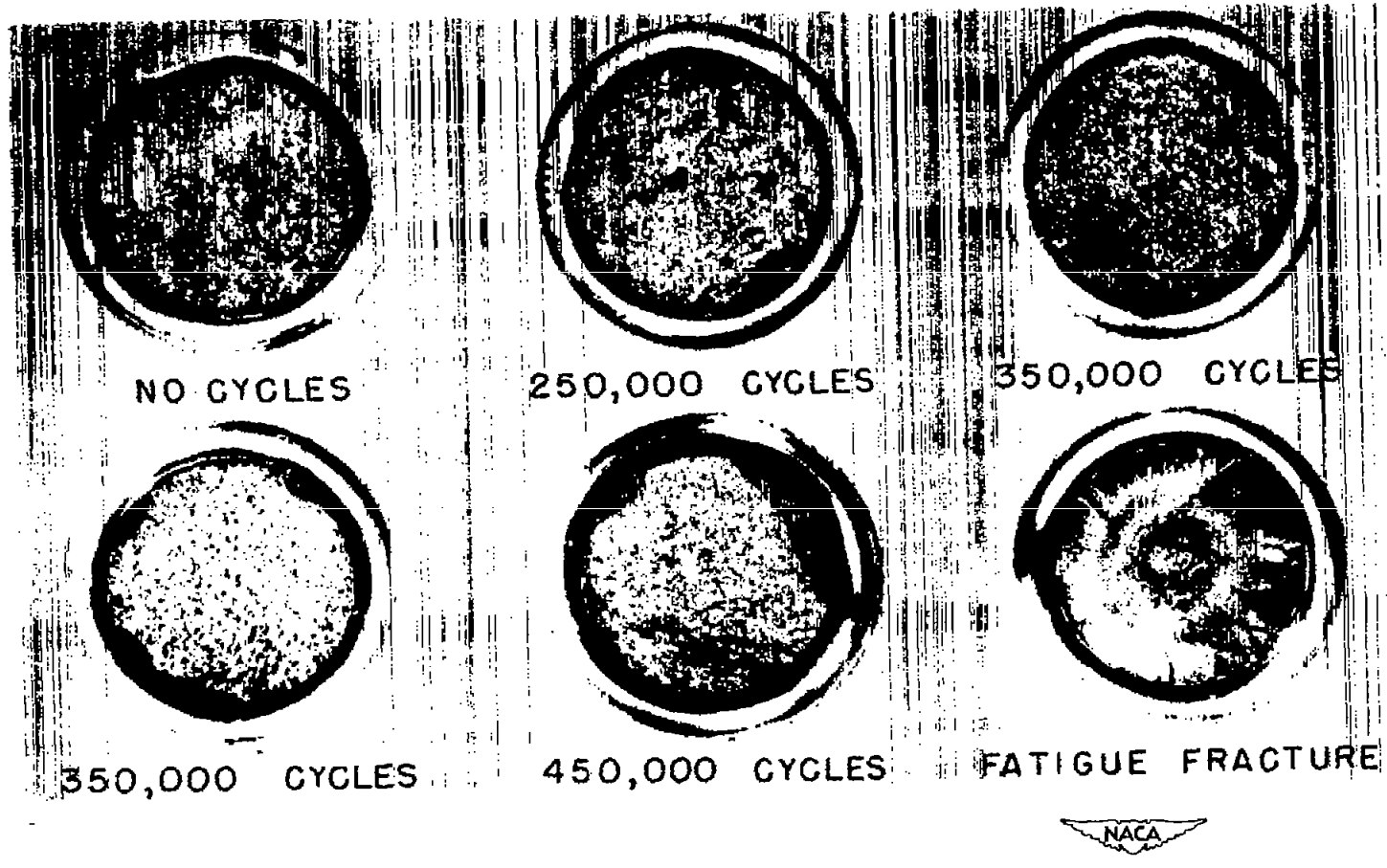

(a) SAE 4130 steel; nominal fatigue bending stress, 46,000 psi.

Figure 12.- Typical views of slow-bend fractures of U-notched specimens after various cycles of fatigue stressing. Notch, 1/16 inch deep with 1/16-inch radius.

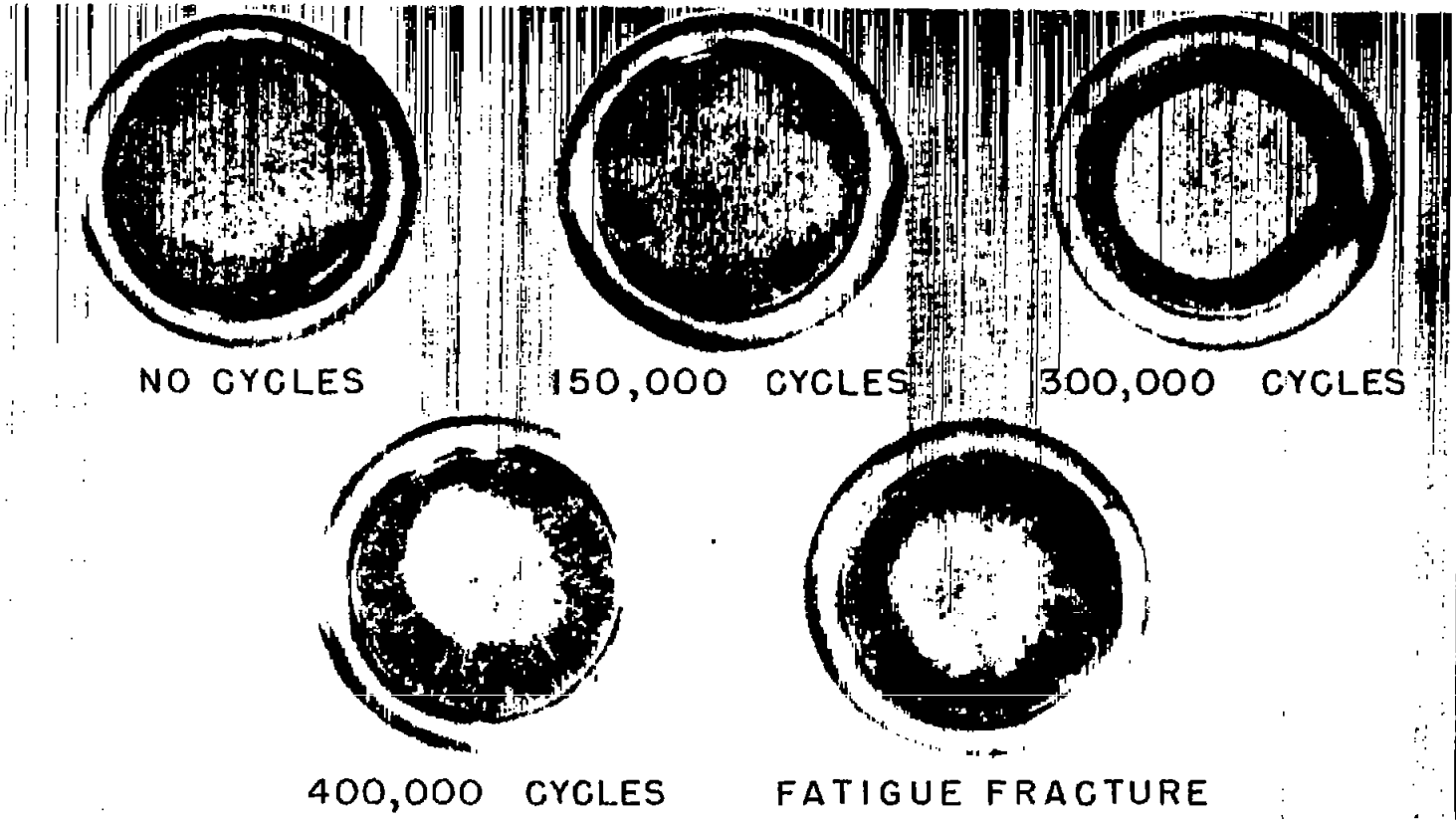

(b) 24S-T4 aluminum alloy; nominal fatigue bending stress, 26,000 psi.

Figure 12.- Continued.

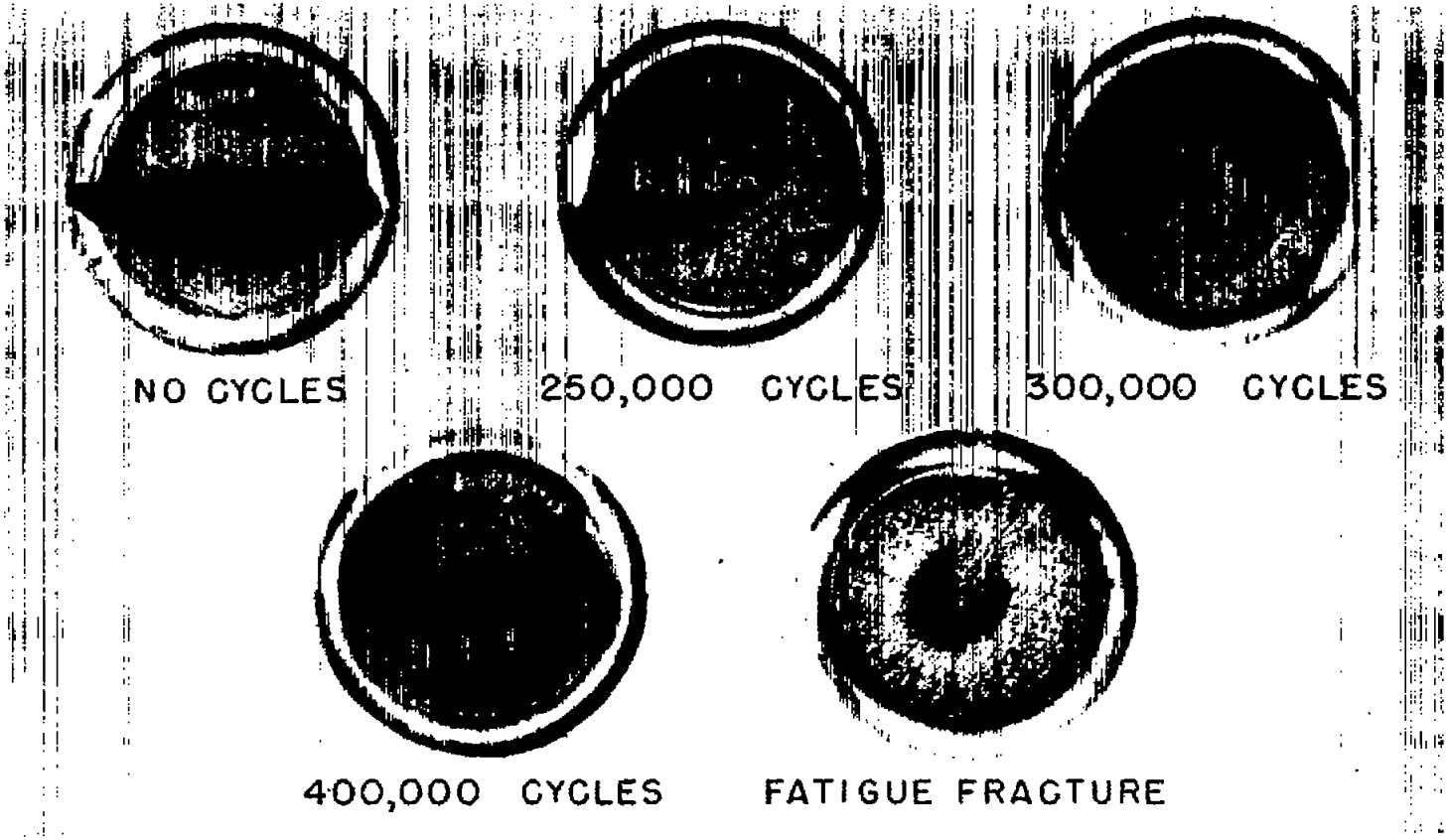

(c) 75S-T6 aluminum alloy; nominal fatigue bending stress, 25,000 psi.

Figure 12.- Concluded.

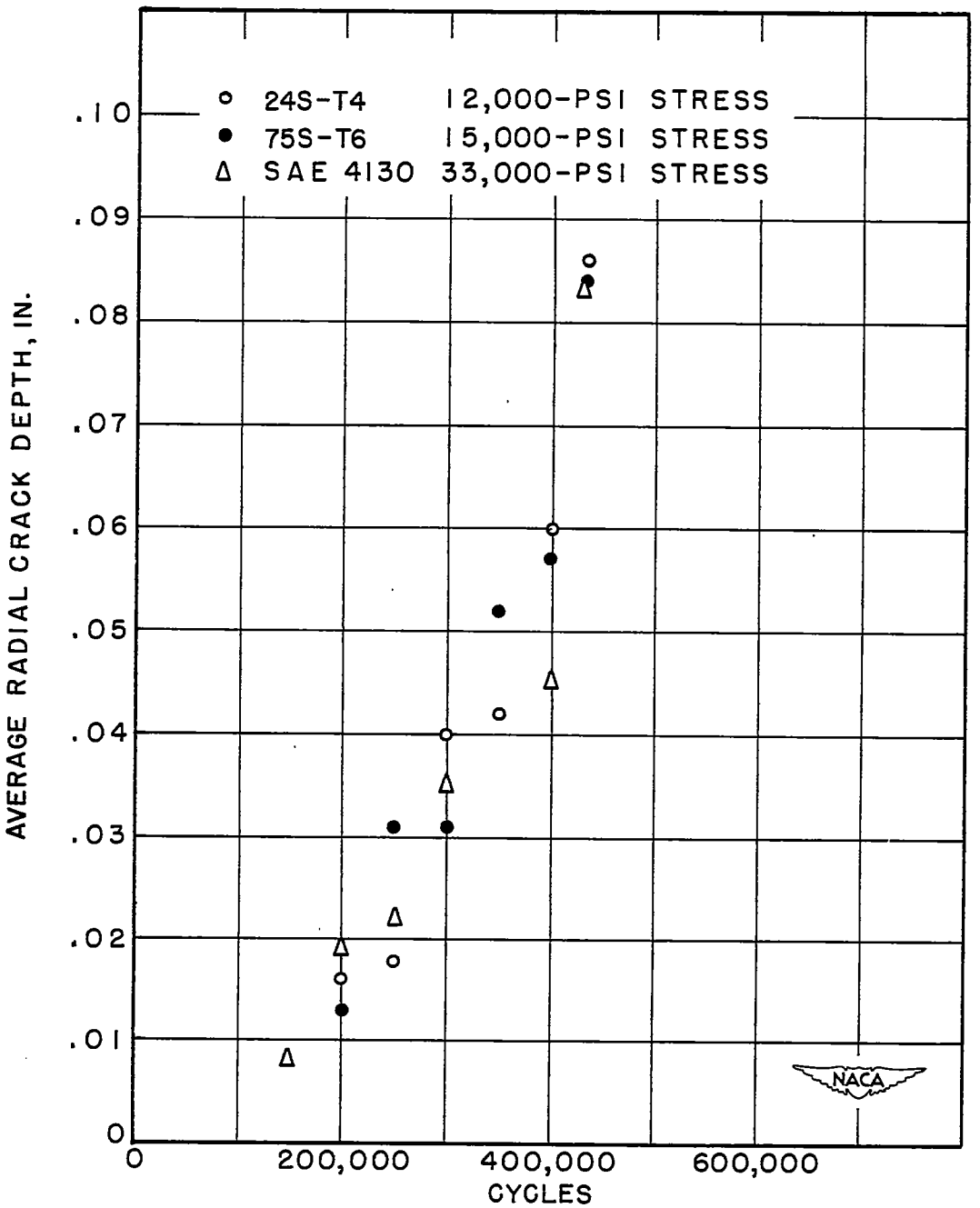

Figure 13.- Average radial crack depth for different numbers of cycles. Approximate fatigue life, 450,000 cycles at respective stress levels. V-shaped notch, 1/16 inch deep with 0.01-inch radius.

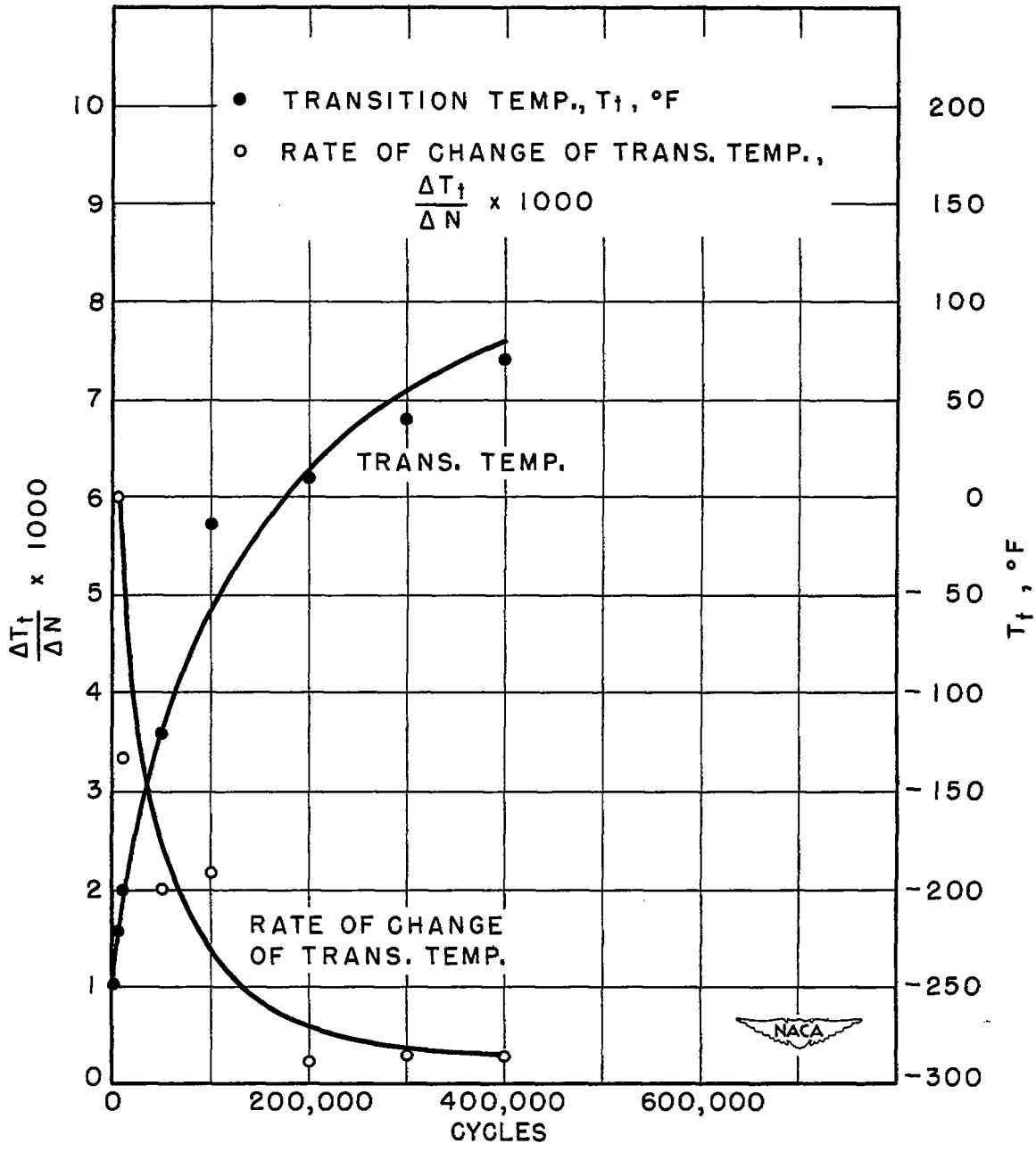

(a) V-notched specimens. Notch, 1/16 inch deep with 0.01-inch radius.

Figure 14.- Transition-temperature values for SAE 4130 steel after various prior cycles of fatigue stressing.

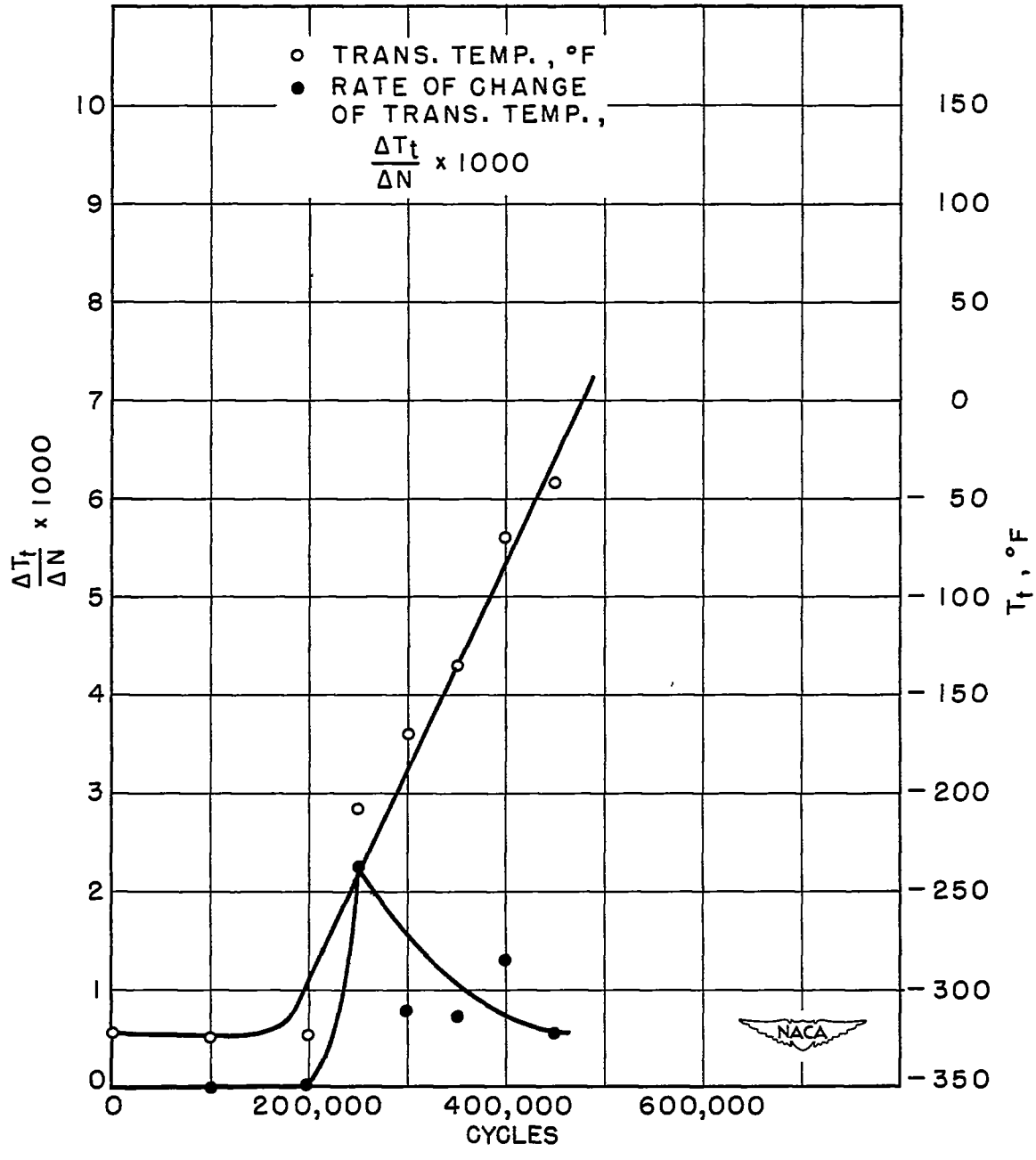

(b) U-notched specimens. Notch, 1/16 inch deep with 1/16-inch radius.

Figure 14.- Concluded.

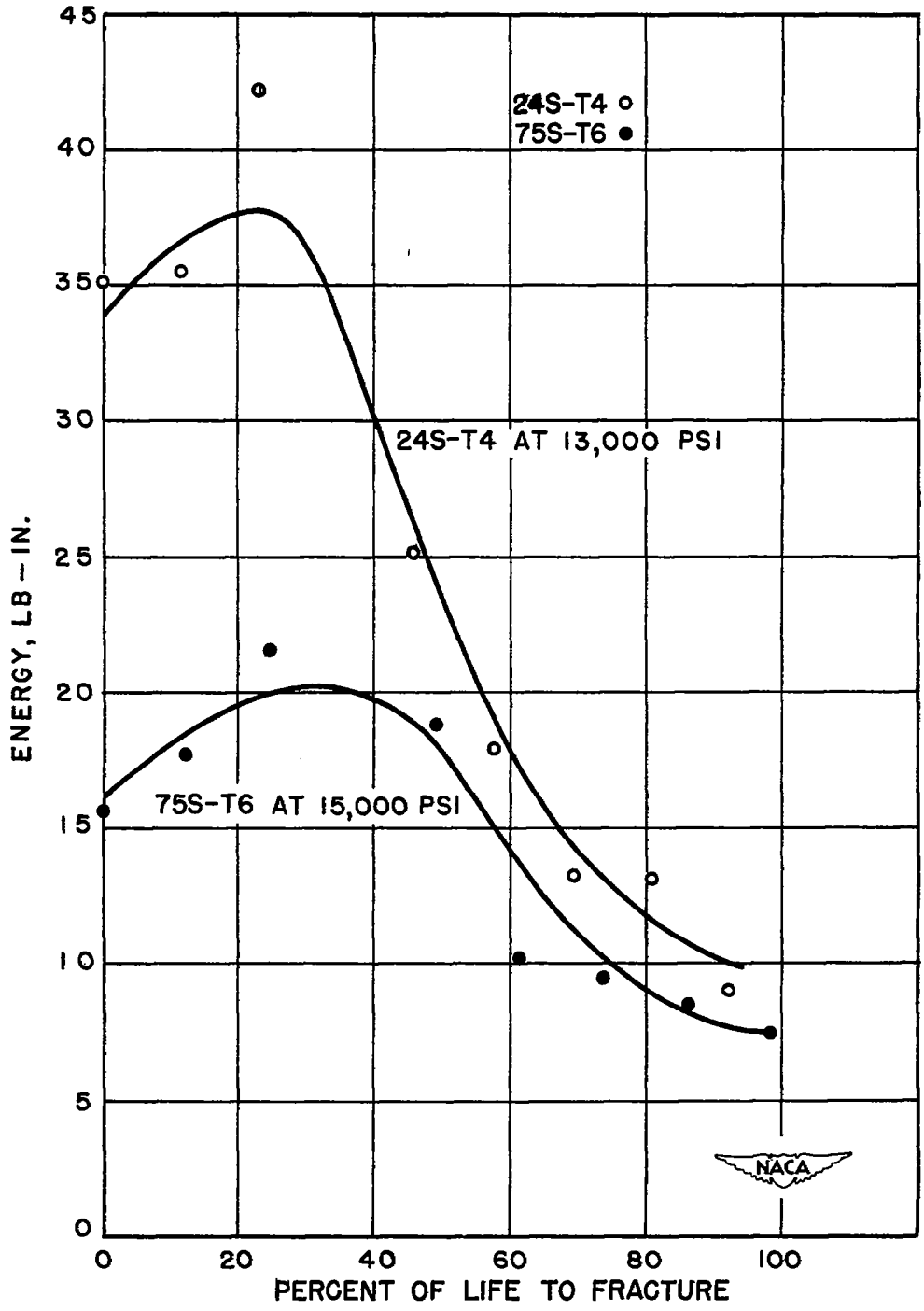

(a) Slow-bend tests at -320° F.

Figure 15.- Average energy to fracture for V-notched specimens of 24S-T4 and 75S-T6 aluminum alloys after prior cycles of fatigue stressing. Approximate life to fracture, 450,000 cycles. Notch, 1/16 inch deep with 0.01-inch radius.

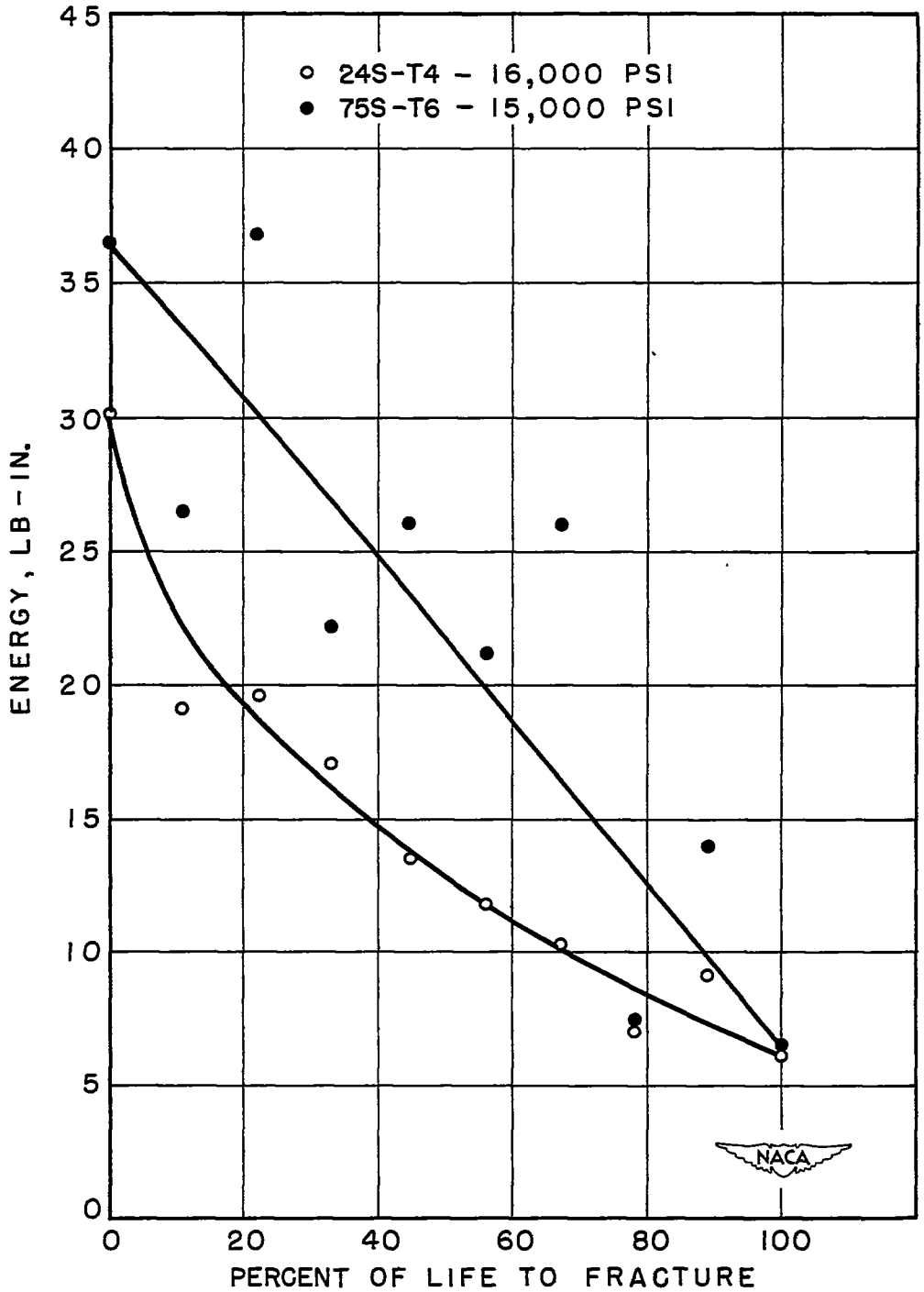

(b) Slow-bend tests at 0° F.

Figure 15.- Concluded.

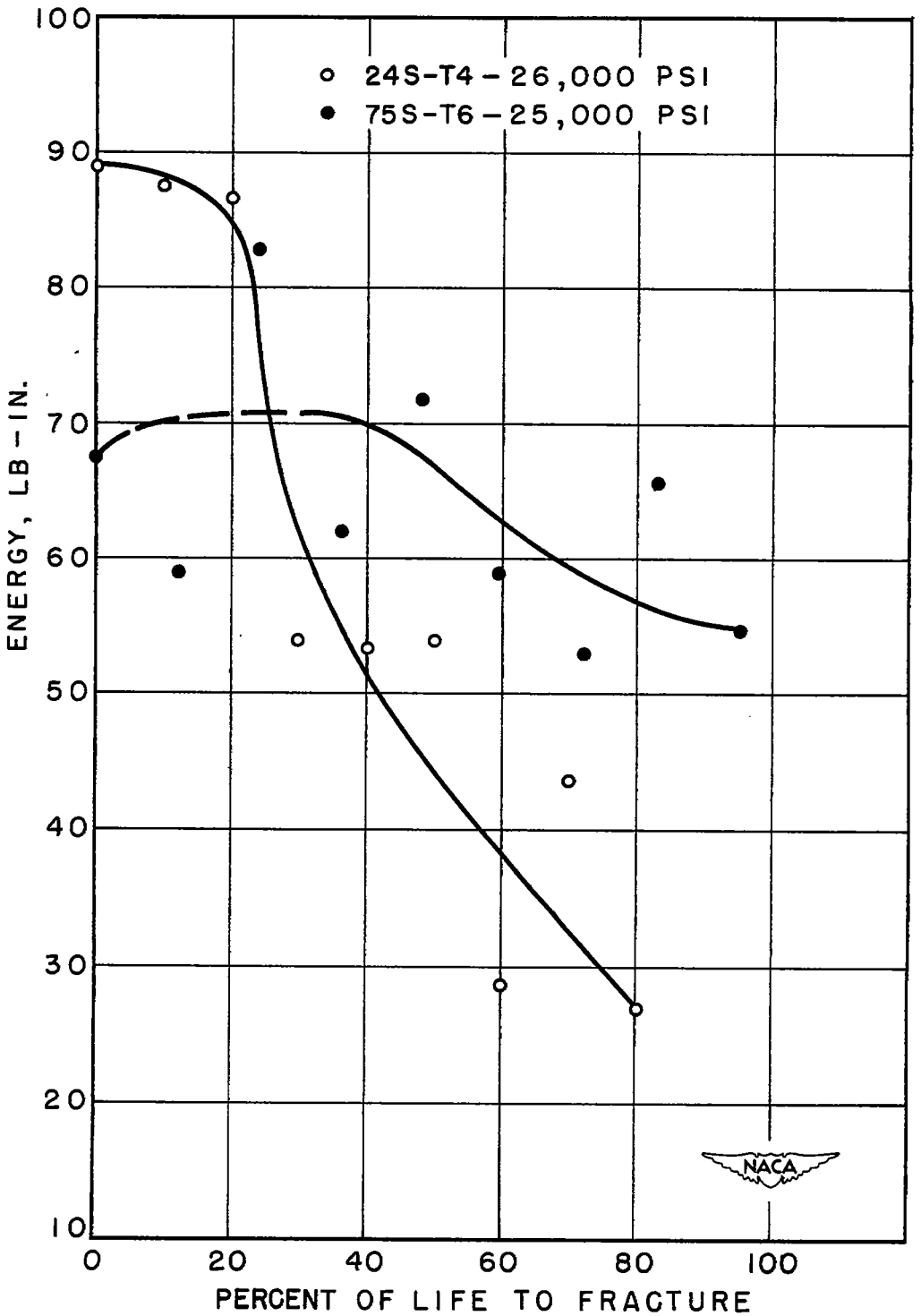

Figure 16.- Average energy to fracture at -320° F for U-notched specimens of 24S-T4 and 75S-T6 aluminum alloys after prior cycles of fatigue stressing. Approximate life to fracture, 450,000 cycles. Notch, 1/16 inch deep with 1/16-inch radius.

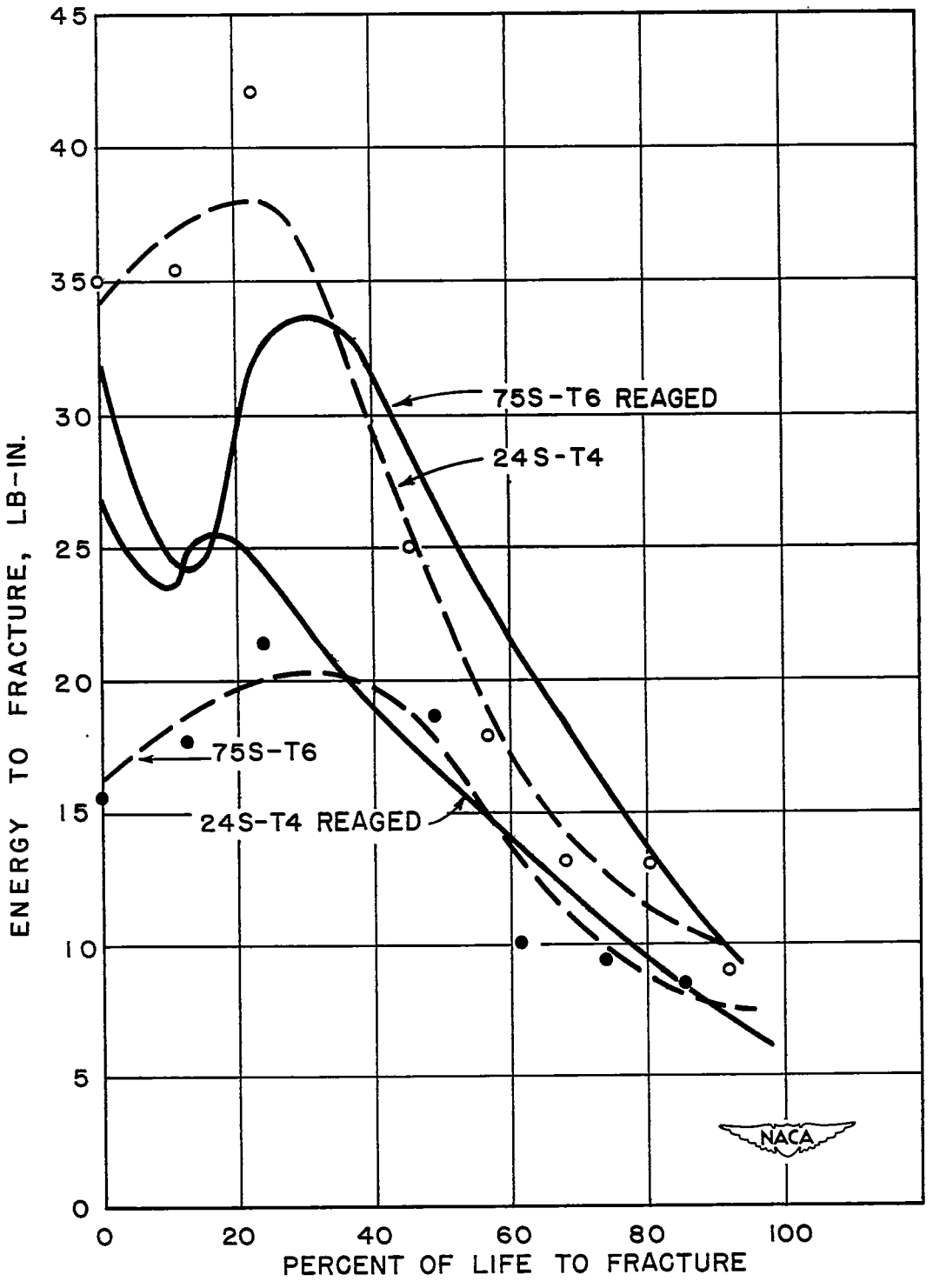

Figure 17.- Comparison of curves of average energy to fracture at -320° F for V-notched fatigue specimens of 24S-T4 and 75S-T6 aluminum alloys after reaging with those for specimens of the alloys in as-received condition. Notch, 1/16 inch deep with 0.01-inch radius.

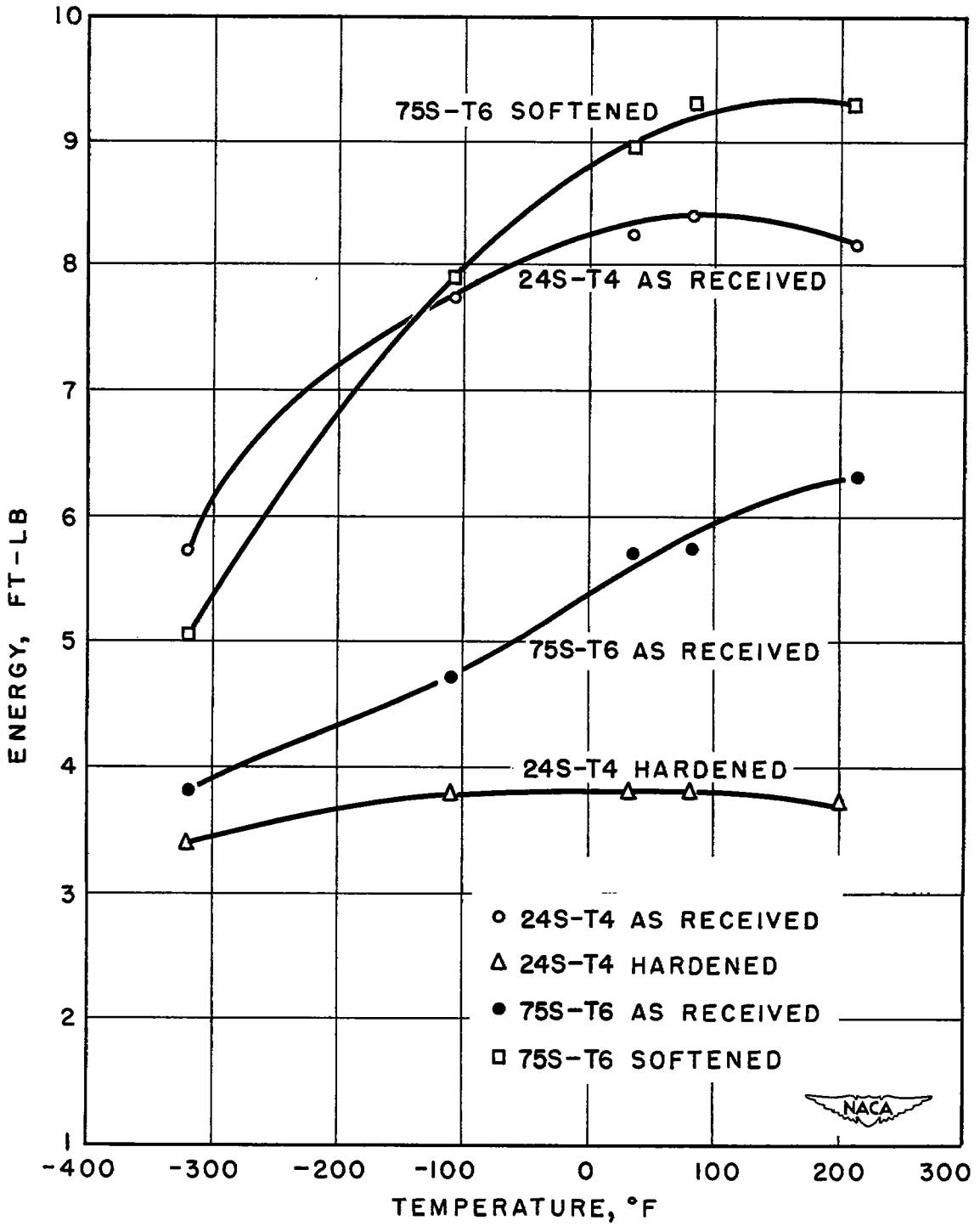

Figure 18.- Charpy impact test results.

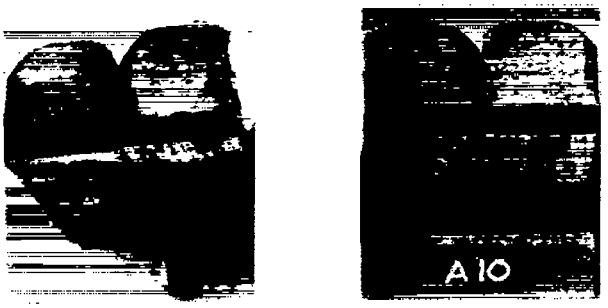

-320° F Room temperature

(a) 24S-T4 as received.

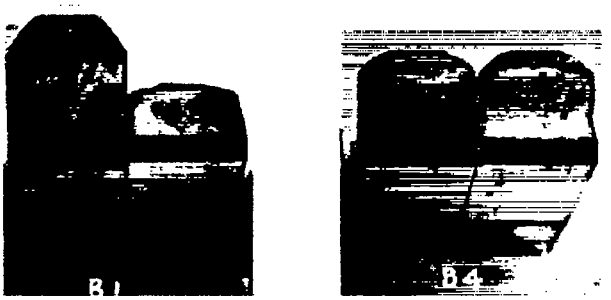

-320° F -110° F

(b) 75S-T6 as received.

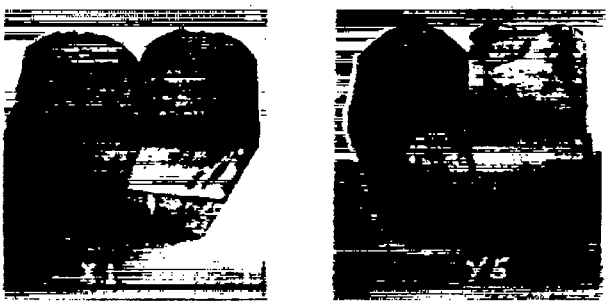

24S-T4, -320° F 75S-T6, 32° F

(c) Heat-treated.

Figure 19.- Typical end views of broken V-notched specimens tested in Charpy impact.

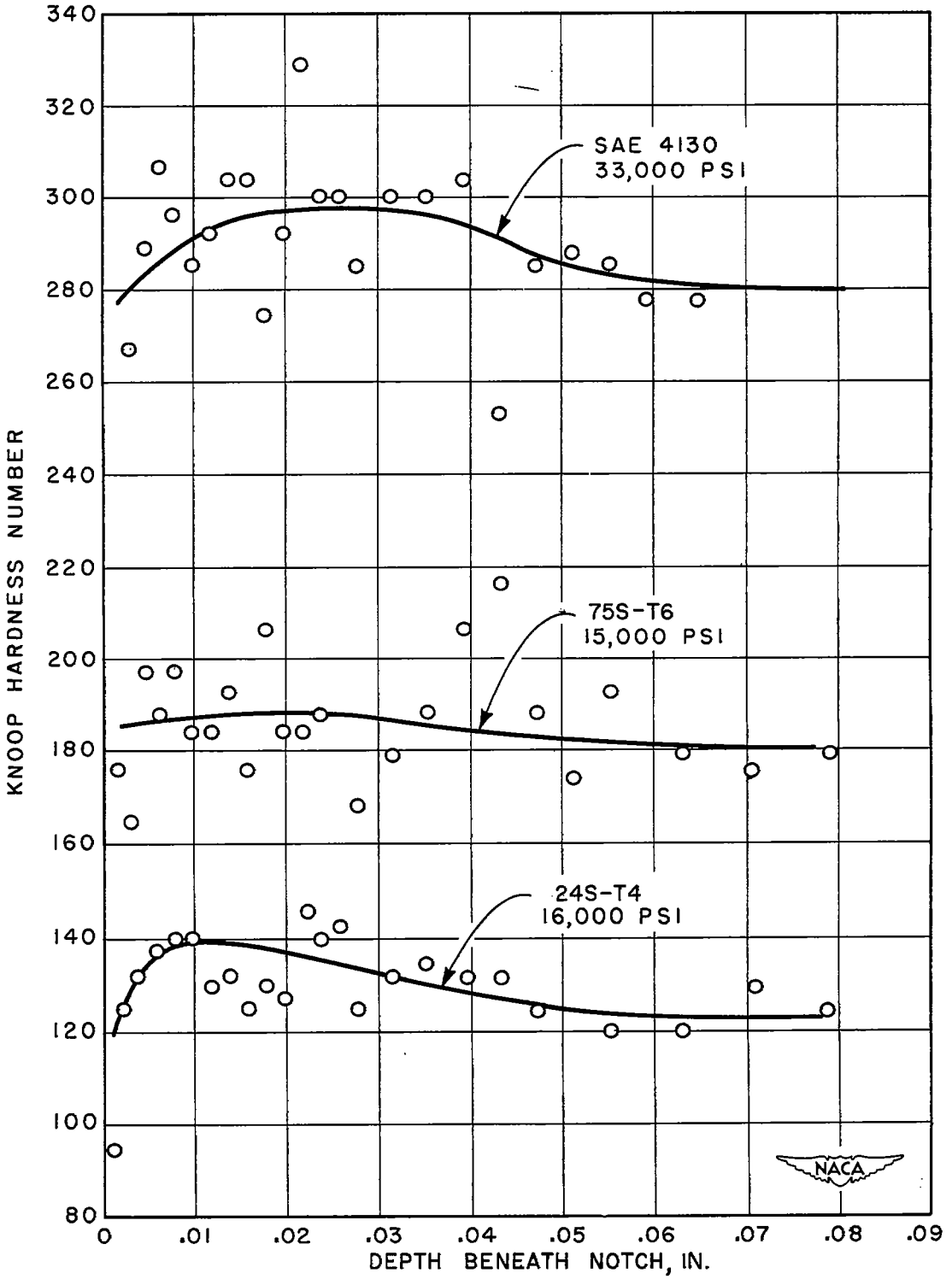

Figure 20.- Microhardness survey of V-notched fatigue specimens subjected to 100,000 cycles of stressing. Approximate fatigue life, 450,000 cycles at respective stress levels. Notch, 1/16 inch deep with 0.01-inch radius.

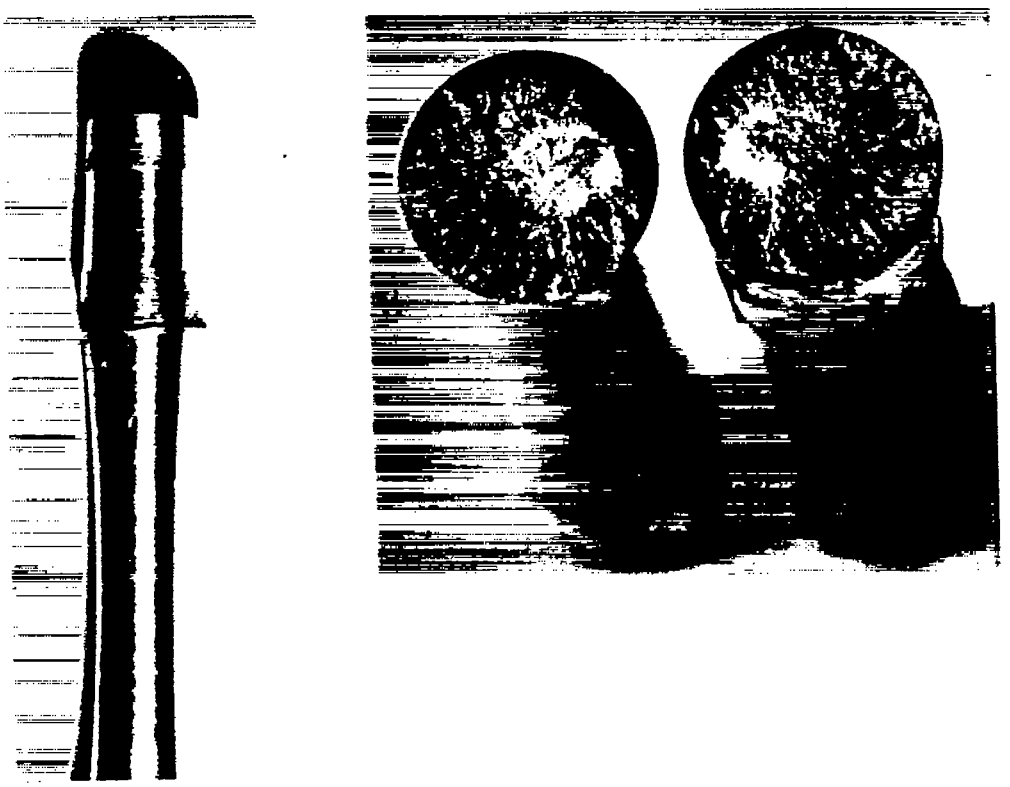

Figure 21.- Views of failure caused by fretting corrosion in chuck for unnotched specimen of 75S-T6 aluminum alloy. Nominal fatigue stress level, 22,000 psi; fracture at 10,616,000 cycles.

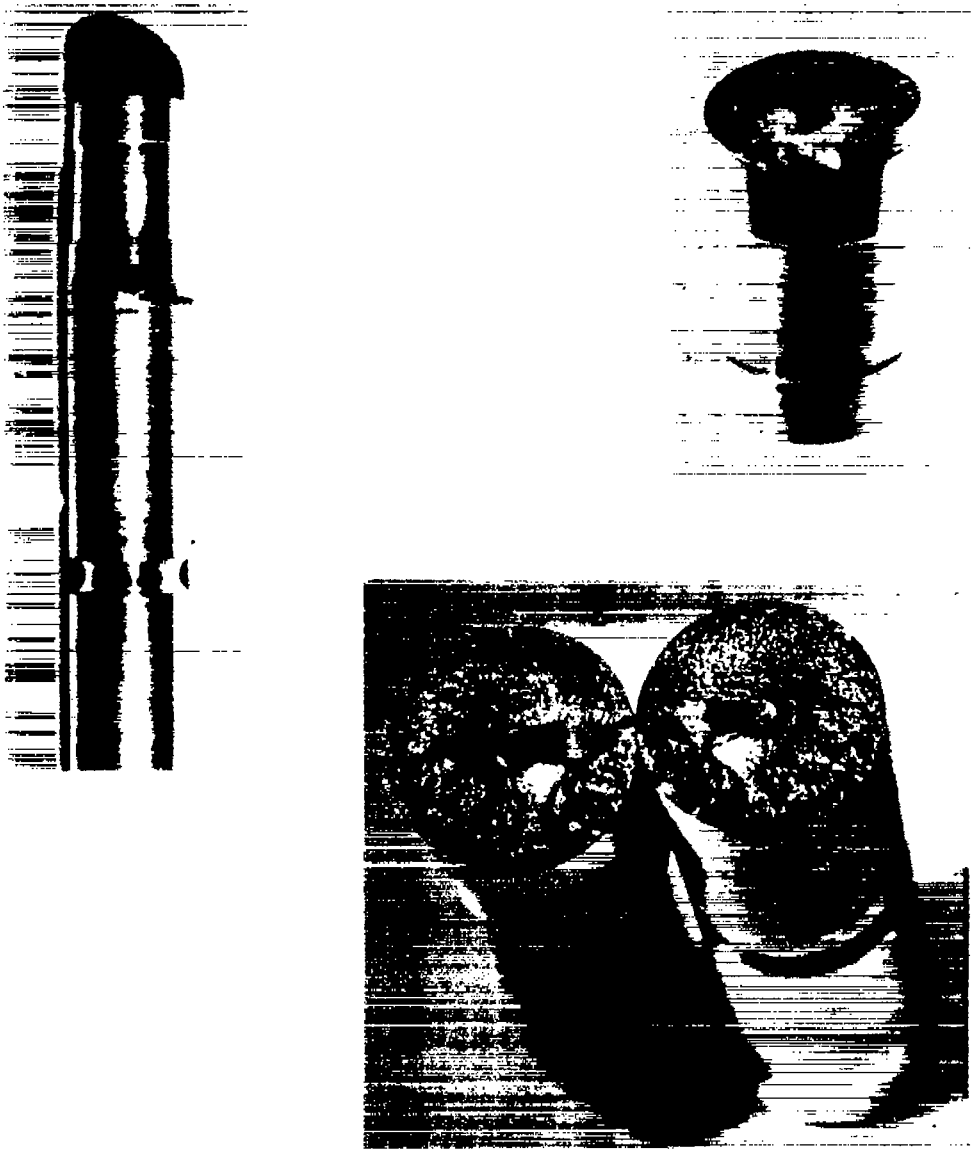

Figure 22.- Views of failure caused by fretting corrosion in chuck for U-notched specimen of 75S-T6 aluminum alloy. Notch, 1/16 inch deep with 1/16-inch radius. Nominal fatigue stress level, 19,000 psi; fracture at 7,700,000 cycles.

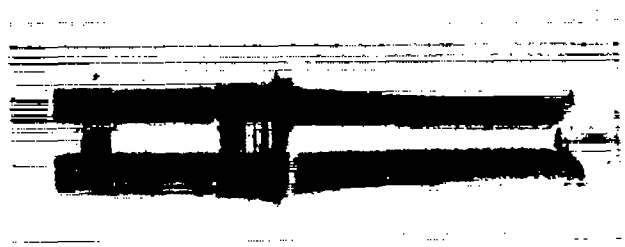

(a) Unnotched.

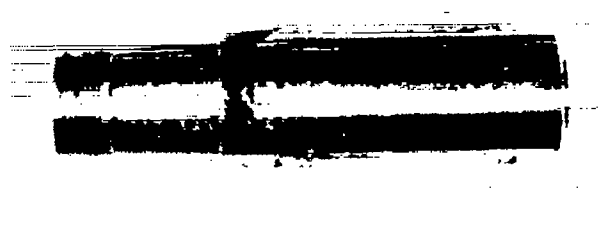

(b) Notched. V-shaped notch, 1/16 inch deep with 0.01-inch radius.

Figure 23.- Views of fatigue specimen of 24S-T4 aluminum alloy as received with fretting occurring in chuck but not causing failure.

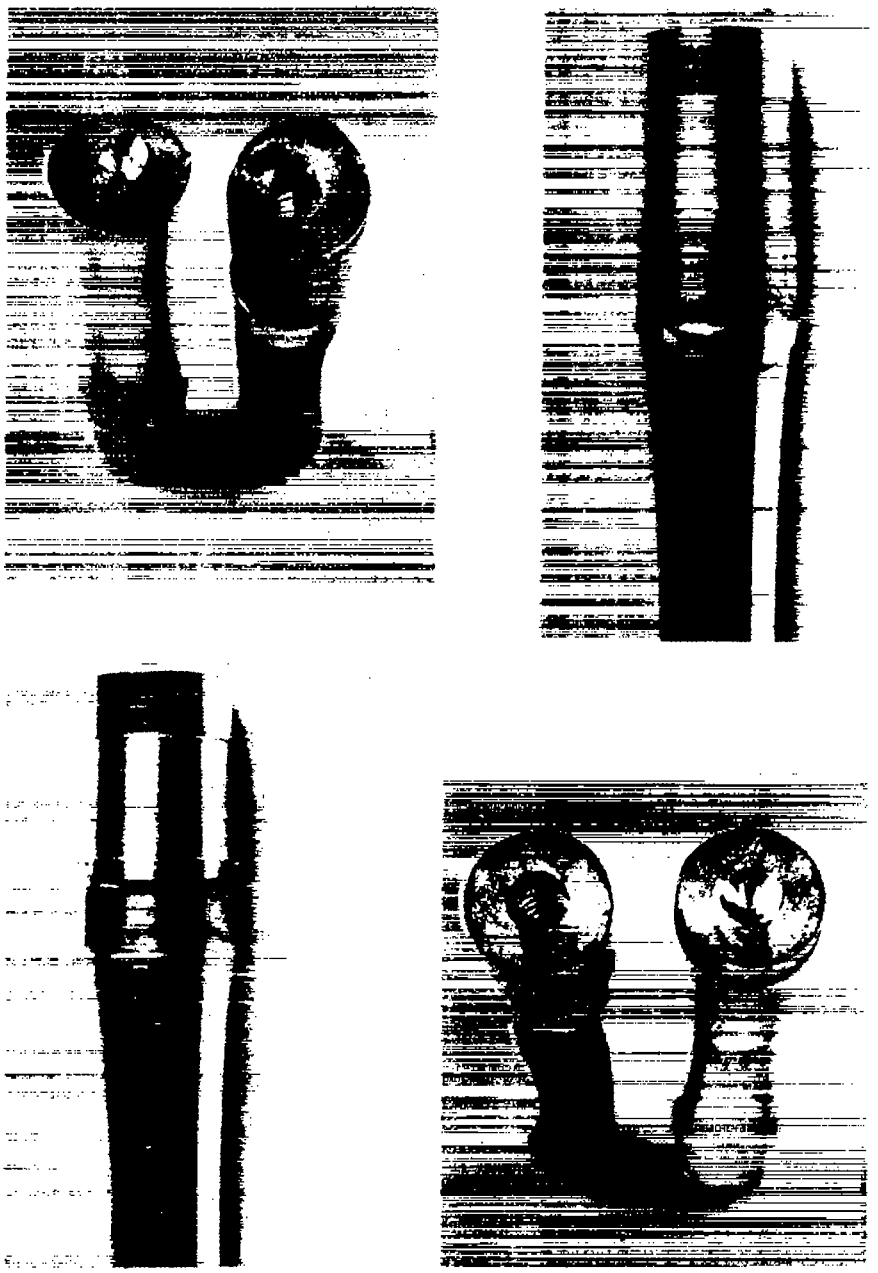

Figure 24.- Views of failures caused by fretting corrosion in chucks for rehardened, unnotched specimens of 24S-T4 aluminum alloy.

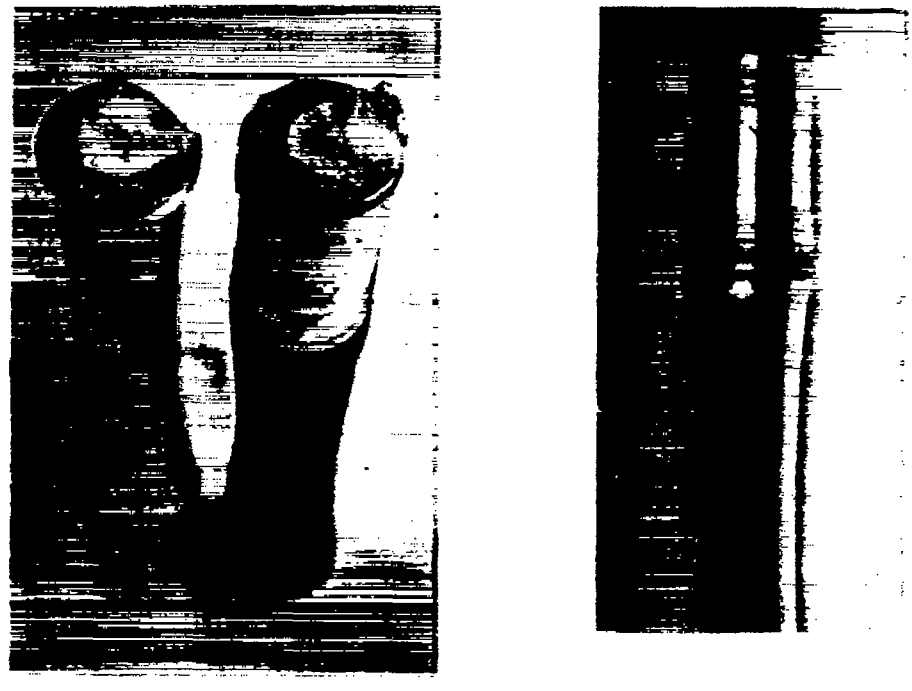

Figure 25.- Views of failure caused by fretting corrosion in chuck for softened, unnotched specimen of 75S-T6 aluminum alloy.

NACA-Langley - 5-3-55 - 100